REPORT DOCUMENTATION PAGE

Form Approved
OMB No. 0704-0188

1. REPORT DATE *(DD-MM-YYYY)*	**2. REPORT TYPE**	**3. DATES COVERED** *(From - To)*
08-11-2012	Final	Aug. 2009-Aug. 2012

4. TITLE AND SUBTITLE
Low Complexity Track Initialization and Fusion for Multi-Modal Sensor Networks

5a. CONTRACT NUMBER
W911NF-09-2-0041

5b. GRANT NUMBER

5c. PROGRAM ELEMENT NUMBER

6. AUTHOR(S)

Qiang Le

5d. PROJECT NUMBER

5e. TASK NUMBER

5f. WORK UNIT NUMBER

7. PERFORMING ORGANIZATION NAME(S) AND ADDRESS(ES)

Hampton University
100 E QUEEN ST
HAMPTON, VA, 23668-0001

8. PERFORMING ORGANIZATION REPORT NUMBER

9. SPONSORING / MONITORING AGENCY NAME(S) AND ADDRESS(ES)

US ARMY RDECOM ACQ CTR - W911NF
4300 S. MIAMI BLV. DURHAM NC 27703

10. SPONSOR/MONITOR'S ACRONYM(S)

ARL

11. SPONSOR/MONITOR'S REPORT NUMBER(S)

12. DISTRIBUTION / AVAILABILITY STATEMENT

Approved for public release, distribution unlimited

13. SUPPLEMENTARY NOTES

14. ABSTRACT
The objective of the project is to undertake research and development in the area of wireless sensor networks to provide an effective and affordable solution in support increasing requirements for reconnaissance and surveillance. A wireless sensor network, such as unattended ground sensors (UGS) network represents a set of inexpensive sensors of various types (modes) that provide an effective and affordable solution for battlefield surveillance. For example, acoustic sensors could obtain bearing angles of targets, and proximity sensors report the presence or absence of targets within their sensing ranges. The ultimate goal of this research is to explore fundamental performance bounds that determine how well a sensor network can resolve and localize multiple targets as a function of the operating parameters such as sensor density, the threshold settings, and the spacing between the targets. The major contribution of this project is the development of the particle-based probability density (PHD) filter for binary measurements using proximity sensors.

15. SUBJECT TERMS
proximity sensors, PHD filter, multiple target tracking

16. SECURITY CLASSIFICATION OF:			**17. LIMITATION OF ABSTRACT**	**18. NUMBER OF PAGES**	**19a. NAME OF RESPONSIBLE PERSON**
a. REPORT	**b. ABSTRACT**	**c. THIS PAGE**			Qiang Le
Unclassified	Unclassified	Unclassified		23	**19b. TELEPHONE NUMBER** *(include area code)* 757-727-5557

Final Report

Low Complexity Track Initialization and Fusion for Multi-modal Sensor Networks

Principal Investigator: Dr. Qiang Le
Hampton University

The objective of the project is to undertake research and development in the area of wireless sensor networks to provide an effective and affordable solution in support increasing requirements for reconnaissance and surveillance. A wireless sensor network, such as unattended ground sensors (UGS) network represents a set of inexpensive sensors of various types (modes) that provide an effective and affordable solution for battlefield surveillance. For example, acoustic sensors could obtain bearing angles of targets, and proximity sensors report the presence or absence of targets within their sensing ranges. The ultimate goal of this research is to explore fundamental performance bounds that determine how well a sensor network can resolve and localize multiple targets as a function of the operating parameters such as sensor density, the threshold settings, and the spacing between the targets. The major contribution of this project is the development of the particle-based probability density (PHD) filter for binary measurements using proximity sensors.

This three year works is summarized in six publications: Aerospace 2010 [1] and Fusion 2010[2]. Army Science 2010[3], Aerospace 2011 [4], SPIE 2011[5], and TAES 2012[6].

The Aerospace 2010 works presents the maximum likelihood localization (ML) algorithm for multi-target localization using proximity-based sensor networks. Proximity sensors simply report a single binary value indicating whether or not a target is near. The ML approach requires a hill climbing algorithm to find the peak, and its ability to find the global peak is determined by the initial estimates for the target locations. This paper investigates three methods to initialize the ML algorithm: 1) centroid of k-means clustering, 2) centroid of clique clustering, and 3) peak in the 1-target likelihood surface. To provide a performance bound for the initialization methods, the paper also considers the ground truth target positions as initial estimates. Simulations compare the ability of these methods to resolve and localize two targets. The simulations demonstrate that the clique clustering technique outperforms k-means clustering and is nearly as effective as the 1-target likelihood peak methods at a fraction of the computational cost.

The Fusion 2010 works documents our initial attempt to determine the operating parameters of a proximity sensor network to achieve a specified probability of resolution at a specified target separation r_s. The probability of resolution is derived by considering three necessary conditions to resolve two targets. These conditions consist of 1) node proximity to the targets, 2) sufficient number of detections from nodes close to the target, and 3) the existence of the “between" node that cannot detect either target. These conditions lead to a design strategy that determines the necessary sensor density and threshold settings to achieve the desired P_r for a given r_s. Simulations demonstrate that at the designed sensor density and threshold values, the actual percentage of targets resolved achieves the desirable level of resolution for moderate to large target separations.

Army Science 2010work documents our initial investigations on multiple target tracking filters in proximity sensor networks. To this end, we implement a PHD filter and compare it to a clairvoyant PF filter. During the measurement update, the filters do not associate targets with the binary measurements due to the fact that the response of a binary sensor is intertwined with the location of all targets. The simulations that compare the PHD to clairvoyant processing demonstrate the feasibility of the PHD to

both estimate the number of targets as well as estimate their target states. One useful feature of the PHD filter is that it considers various combinations of PHD particles when performing the measurement update. The advantage of this feature was demonstrated via the simulations.

Aerospace 2011work further documents our investigation of multiple target tracking filters in proximity sensor networks. To this end, we implemented a particle-based PHD filter and compared it to ClusterTrack, a clustering-based particle filter. The simulations that compare the PHD to the ClusterTrack method demonstrate the advantages of PHD method. For the 2-D tracking case, the localization accuracy of the PHD is far better than that of the ClusterTrack. Unlike ClusterTrack, the PHD is able to estimate the number of targets. The advantages of the PHD may be due to the fact that it is based principled Bayesian approach; whereas the ClusterTrack is more ad-hoc in its design.

This SPIE 2011 work investigates how the sensor density, sensing range, and target separation affect the ability of the PHD filter to estimate the number of targets in the scene and to localize these targets (as measured by four different metrics). Two possible measurement models are considered. The disc model assumes target detection within a sensing radius, and the probabilistic model assumes $1/r^2$ propagation decay of the source signal so that the probability of detection decreases with range r. The simulations demonstrate the simplistic disc model is inadequate for the PHD filter to estimate the number of targets, and the filter for the disc model exhibits difficulty to localize widely separated targets for low sensor densities. On the other hand, the more realistic probabilistic model leads to a PHD filter that can accurately estimate the number and locations of targets even for small target separations.

The TAES 2012 work documents our investigation of multiple target tracking filters in proximity sensor networks. To this end, we developed a novel formulation of the PHD filter for proximity sensors. We compared the PHD against two clairvoyant filters that assume the number of targets is known a priori. For measuring the localization errors, we considered a measure that attempts to separate out the effects of cardinality errors. The simulations show the advantages of the crossover feature in the PHD.

Two possible measurement models were considered: the disc and probabilistic, so that two model matching cases and two model mismatching cases were considered. While the disc model has wide appeal, the probabilistic model better represents the phenomenology that dictates how sensors respond to target signals. The simulations demonstrate that the PHD filter would be unable to accurately estimate the number of targets if the disc model was assumed in the measurement update. This is the case because the hypothesis that explains the pattern of detection reports is not unique. On the other hand, the PHD is accurate when using the probabilistic model in the measurement update because of the uniqueness of the best hypothesis to explain the pattern of detection reports.

The unique hypothesis emerges because it is assumed that the radiating power of each target is a fixed and known quantity. In reality, one would expect that this power fluctuates from target to target. If these fluctuations are unbounded, the probabilistic model becomes completely ambiguous, and it would be impossible for the PHD filter to accurately estimate the number of objects in the scene. However, we expect that these fluctuations are bounded. Future work will investigate how allowing for bounded spread of target power levels will affect the performance of the PHD filter. Other future work will investigate better dynamical models to improve the tracking performance including target motion and birth/death models, and other cluster methods for closely spaced targets.

Finally, the new PHD filter in this paper uses a profoundly different measurement model than the traditional PHD filter. When the sensor measurements are statistically independent conditioned on the target hypothesis as in this paper, the multisensor version of the PHD is straightforward. However, for the traditional PHD filter, the "exact" multisensor version is very cumbersome to implement. Usually, approximations are incorporated in the multisensor implementation of the traditional PHD. These approximations are necessary due to the constraints that a measurement corresponds either to one unique target or clutter. Actually, the measurements are usually derived from raw signals through signal processing, e.g., direction of arrival estimation. As an alternative, the new PHD method could easily be modified to consider the likelihood of raw signals given the target hypotheses. The new PHD method does suffer from approximations in the particle implementation of the multiobject target density. On the other hand, approximations of the PHD for sensor fusion also lead to performance loss. Future work can investigate whether the new PHD method operating over raw signals from multiple sensors has utility compared to multiple sensor implementation of the traditional PHD method.

Since FY2010 and FY2011 annual reports already include Aerospace 2010 [1] and Fusion 2010[2]. Army Science 2010[3], Aerospace 2011 [4], SPIE 2011[5] as attachments. In this final report, only TAES [12] is included as attachment.

Publications

1. Q. Le and L.M. Kaplan, "Target localization using proximity binary sensors," Proceedings of IEEE Aerospace conference, Big Sky, MT, Mar. 2010.
2. Q. Le, and L.M. Kaplan, "Design of Operation Parameters to resolve Two Targets using Proximity Binary Sensors " in 13th International Conference on Information Fusion, July, 2010, Edinburgh, UK.
3. Q. Le, and L. M. Kaplan, "Multitarget Tracking using Proximity Sensors," Proceedings of Army Science Conference, Orlando, FL, Nov. 2010.
4. Q. Le, and L. M. Kaplan, "Target Tracking using Proximity Binary Sensors," Proceedings of IEEE Aerospace Conference, Big Sky, MT, Mar. 2011.
5. Q. Le, and L. M. Kaplan, "Effects of Operation Parameters on Multitarget Tracking in Proximity Sensor Networks," Proceedings of SPIE Conference, Orlando, FL, April, 2011.
6. Q.Le, and L.M.Kaplan, "Probability Hypothesis Density-Based Multitarget Tracking using Proximity Sensors," accepted by IEEE Transaction on Aerospace and Electronics Systems in Sept. 2012

Probability Hypothesis Density-Based Multitarget Tracking for Proximity Sensor Networks

Qiang Le and Lance M. Kaplan

***Abstract*—This paper investigates the feasibility of a mesh network of proximity sensors to track targets. In such a network, the sensors report binary detection/nondetection measurements for the targets within proximity. This work proposes a new probability hypothesis density (PHD) filter and its particle implementation for multiple target tracking in a proximity sensor network. The performance and robustness of the new method is evaluated over simulated matching and mismatching cases for the sensor models. The simulations demonstrate the utility of the PHD filter to both track the number of targets and their locations.**

***Index Terms*—proximity sensors, PHD filter, multiple target tracking.**

I. Introduction

Proximity (or binary) sensors are simple, low power devices that report whether or not they detect a target. Typically, these sensors are used to cue more sophisticated sensors that require more power in order to classify and track the targets. This paper investigates the feasibility of a mesh network of proximity sensors to track targets. In such a network, the no-detection report is as valuable as a detection report. Previous work has revealed the potential of target localization and tracking for a single target [1], [2], [3], or for a ideal disc sensing model [4], [5], [6], [7], [8] where [7], [8] does consider multiple target tracking. There are two models to describe the behavior of the proximity sensor that drive localization algorithms. Many approaches are based on the disc model that assumes a sensor detects a target when and only when the target's distance to the sensor is below a sensing radius [4], [5], [6], [7]. The disc model ignores physical phenomenology such as the additive effects of the energy radiating from multiple targets will extend the sensing range. Other approaches use a probabilistic model for the sensors that is based on a physical energy loss as the energy is radiated from each of the targets [1], [2].

For multiple-target tracking, Singh, *et al.*, proposed *ClusterTrack*, which is a clustering-based particle filter approach to track targets based on the disc model [7], [8]. While ClusterTrack can track targets in real-time, the method can only localize all targets when operating in a batch mode where measurements from later points in time are employed to localize tracks at a given time. Furthermore, it assumes the number of targets in the scene does not change over the batch processing interval. He, *et al.* proposed a multitarget tracking approach using a probabilistic model [9]. However, the method only tracks the presence of targets within cells of a grid. On the other hand, the focus of our work is to localize and track multiple targets over continuous states including target location. Our recent work presents a maximum likelihood (ML) localization algorithm for multitarget localization when the number of targets is known [10]. This work extends [10] by considering the more general application of target tracking when the number of targets is unknown. To this end, the likelihood function is integrated into a particle filter implementation of a modified version of the probability hypothesis density (PHD) filter as described in [11].

Traditional particle filter approaches in multiple target tracking must employ measurement-to-track association techniques to ensure as much as possible that target state estimates are not contaminated by wrong measurements [12]. In contrast, the PHD filter introduced in [11] is able to "sweep the association issue under the rug" because the PHD is actually tracking the density of target presence, i.e., PHD, and not actual point targets. The estimated number of targets in the scene is simply the integral of the PHD over the target states. However, extraction of estimates of the target locations requires a clustering method. The issues of how to transform the PHD into point target estimates are discussed in [13].

The applications of the PHD filter have been seen in sonar, visual, and radar tracking [13], [14], [15], [16], [17], [18]. For example, [14], [15] implemented the PHD filter to identify the underwater obstacles that would need to be avoided in navigation using forward-scan sonar images. In [16], the PHD filter was employed to track a random number of pedestrians in image sequences and derive their location sequences. In [17], the PHD filter was applied to target tracking using both range and Doppler measurements. More generic PHD filters are described in [13], [18] that incorporate Cartesian target position measurements directly or through bearing and range measurements. To the best of our knowledge, the PHD filter has not yet been used in proximity-based multiple target tracking.

These PHD filters assume that the measurements are independent and associated to one target. As a result, the measurement update of the PHD has a simple analytical form. This paper takes a more general view that the PHD filter is a sequential Bayesian tracker that is only following the evolution

Q. Le is with the Department of Engineering, Hampton University, Hampton, VA 23668

L. Kaplan is with the US Army Research Laboratory, Adelphi, MD 20783

Research was sponsored by the Army Research Laboratory and was accomplished under Cooperative Agreement Number W911NF-09-2-0041. The views and conclusions contained in this document are those of the authors and should not be interpreted as representing the official policies, either expressed or implied, of the Army Research Laboratory or the U.S. Government. The U.S. Government is authorized to reproduce and distribute reprints for Government purposes notwithstanding any copyright notation herein.

of the first order multitarget moment of the multiobject density no matter the dynamical and measurement models that are incorporated. A motivation for the PHD is that following the multiobject density itself is too cumbersome for practical implementation, e.g., via particle filtering. In this paper, we apply PHD filtering for a mesh network of proximity sensors where the measurements do not directly associate to a single target. As is shown in the next section, the response of the proximity sensor depends on its location relative to the location of all targets within the scene. As a result, the measurements, i.e., the binary outputs of the proximity sensors, are intertwined with all targets. Therefore, tracking with binary sensors requires a modification of the likelihood (measurement) update equation in the original PHD formulation. In this paper, we derive the modified measurement update equation by using the same Bayesian update method as in [11], with the exception that the form for the multisensor/target likelihood is not separable. Unfortunately, the new likelihood update method does not admit a closed form analytical solution. Nevertheless, the numerical computation via particle filtering is straightforward.

This paper is an extension of a series of our earlier conference papers that initially presented our ideas for PHD-based multitarget tracking via a network of proximity sensors. The initial method was introduced in [19], and the method was compared with ClusterTrack in [20]. The ClusterTrack particle filter is to the best of our knowledge the only other method to track multiple targets over a continuous space via proximity sensors. An initial version of the ClusterTrack particle filter was proposed for the disc sensor model and tested on 1-D data in [7]. In [20], we demonstrated that unlike that version of ClusterTrack, the PHD method was able to accurately estimate the number of targets, and the PHD methods were able to better track the targets. In [21], we investigated the performance of the PHD method as a function of sensor density and target separation of two targets. That work demonstrated that the PHD method using the probabilistic sensing model is able to estimate the number of targets and localize them no matter the target separation for sufficient sensor density. This paper expands upon [19], [20], [21] by presenting a more thorough description of the new PHD filter and its particle implementation. Furthermore, this paper includes a new investigation of the performance of the PHD method for both model matching and mismatching conditions. We also compare the PHD methods against the more recent version of ClusterTrack [8]. Furthermore, this paper investigates the tradeoff between the relative weighting on the reliance on prior measurements and current measurements through the use of "innovative" particles.

The paper is as organized as follows. Section II provides details about the proximity sensor model. Then, Section III provides a basic review of finite point processes and presents the new PHD filter for the proximity sensor network and its particle filter implementation. This section also discusses a clairvoyant N-target particle filtering method that provides the baseline to understand the effectiveness of the PHD filter to estimate the number of targets and localize their positions. Simulations are provided in Section IV to characterize the performance of the PHD filter in light of the clairvoyant tracking methods and ClusterTrack. Two sensor model matching cases and two sensor model mismatching cases are considered. Finally, Section V provides concluding remarks.

II. Sensor Model

This section presents two sensing models that describe how the interactions of the targets within a proximity sensor lead to a binary measurement. The probabilistic sensor model taken from [2] considers how the signals radiating from the targets physically manifest into a measurement. The disc model is an idealization that is commonly seen in the literature. While we believe that the probabilistic model is a better representation of how measurements emerge, it is interesting to understand the implication of both models on tracking performance in a proximity sensor network.

A. Probabilistic sensor model

The probabilistic model accounts for the effects of sensor noise so that a sensor will report (or not report) a detection based on some probability of detection. This detection probability goes up as the signal from the targets increases, which happens as targets move closer to the sensor. The probabilistic model used in this paper is taken from [2]. In essence, the model assumes that target signals are uncorrelated so that the power measured at the sensor is the sum of target powers at the sensor plus measurement noise. Specifically, the instantaneous received power p_i, i.e., the power measurement of the i-th sensor at a given point in time, is given by

$$p_i = \sum_{k=1}^{N_t} p_{0,k} \left(\frac{r_{0,k}}{r_{i,k}} \right)^{\alpha} + v_i, \tag{1}$$

where $p_{0,k}$ is the power measured at a reference distance $r_{0,k}$ due to the k-th target, N_t is the total number of targets, $r^t_{i,k}$ is the relative distance between the i-th sensor and the k-th target, α is the attenuation parameter that depends on the transmission medium, and v_i is additive white Gaussian noise, i.e.,

$$v_i \sim \mathbf{N}\left(\mu_v, \sigma_v^2\right).$$

The mean and variance of the error v_i is derived from the zero mean measurement noise of variance σ^2 for the case that the measured power is the result of integrating the square of the measurements over L samples. As shown in [2], [22], integrating over L samples leads to $\mu_v = \sigma^2$ and $\sigma_v^2 = 2\sigma^4/L$. This paper assumes the reference distances $r_{0,k} = r_0$ and target powers $p_{0,k} = p_0$ for all K targets, and r_0 and p_0 are known. As discussed later in this subsection, knowledge of p_0 enables one to infer the number of targets simply from the binary detection reports. Clearly, the assumption that the target signal powers are all equal and known is not realistic, and future work will investigate the relaxation of this assumption.

The i-th sensor measures the received power p_i, processes it locally, and reports a single binary digit: '1' for the presence of one or more targets or '0' for the absence of any target. The decision follows the rule

$$z_i = \begin{cases} 1 & p_i > \lambda, \\ 0 & p_i \leq \lambda. \end{cases} \tag{2}$$

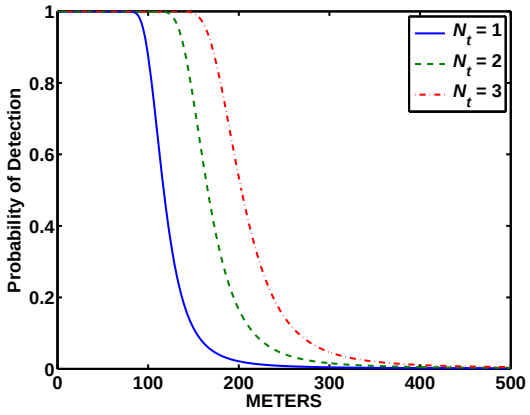

Fig. 1. P_d vs. target distance, where P_{fa}=0.001, $\alpha = 2$, $\sigma = 0.5$, $p_0 = 3000$, $r_0 = 1$m, and $L = 100$.

The probability of false alarm P_{fa} is the probability that z_i exceeds the threshold when $N_t = 0$. For a desired value of P_{fa}, the threshold λ is computed as:

$$\lambda = \sigma_v Q^{-1}(P_{fa}) + \mu_v, \tag{3}$$

where $Q(\cdot)$ is the Q-function

$$Q(x) = \frac{1}{\sqrt{2\pi}} \int_x^\infty e^{-\frac{t^2}{2}} dt.$$

Furthermore, the probability of detection P_d for the chosen threshold (or P_{fa}) at the sensor is a function of the positions of the N_t targets, i.e., $\mathbf{y}_k$, relative to the location of the sensor, i.e., $\mathbf{s}$, as given by

$$\begin{aligned} P_d(\mathbf{s}, [\mathbf{y}_1, \ldots, \mathbf{y}_{N_t}]) &= \text{Prob}(z_i = 1|\text{targets}), \\ &= \text{Prob}(p_i > \lambda|\text{targets}), \\ &= Q\left(\frac{\lambda - \sum_{k=1}^{N_t} p_{0,k} \left(\frac{r_{0,k}}{r_k}\right)^\alpha - \mu_v}{\sigma_v} \right), \end{aligned} \tag{4}$$

where $r_k = \|\mathbf{y}_k - \mathbf{s}\|$. Fig. 1 illustrates P_d as a function of the target distance for various numbers of targets. For the case of a single target, the figure demonstrates that P_d as given by (4) behaves as a sigmoid function that steps down from a value near one to a value near P_{fa} over a transition region from 100m to 200m.

For multiple targets, the addition of the target powers as seen in (4) does extend the sensing range of the sensors as demonstrated in Fig. 1. This fact actually allows for one to infer the number of targets when looking at the distribution of detection reports in a mesh network of proximity sensors. If the targets are far apart, one would expect to see separate clusters of sensors reporting detections around each target. When the targets are near each other, only one cluster emerges. The size of the cluster increases as more targets are in the same vicinity due to the addition of powers in (4), and it is the size of the cluster that provides the clue to the number of targets. The ability to estimate the number of targets depends on having a good handle on the target radiation power $p_{0,k}$. If $p_{0,k}$ is not known, then the number of targets within the cluster of sensing nodes is ambiguous, e.g., is there one loud target or multiple quiet targets? For this reason, we assume in this paper that $p_{0,k} = p_0$. Future work will investigate robustness of this assumption when the targets radiation power is known to fall within a certain range.

B. Disc sensor model

Many papers exploiting proximity sensors assume the *disc* sensor model, where a sensor always detects one or more targets if they are within the detection range r_{eff} and never detects any target if all are further than r_{eff} from the sensor:

$$P_d(\mathbf{s}, [\mathbf{y}_1, \ldots, \mathbf{y}_K]) = \begin{cases} 1 & \exists k, \|\mathbf{y}_k - \mathbf{s}\| \leq r_{eff}, \\ 0 & \text{otherwise.} \end{cases} \tag{5}$$

The disc model ignores the physical process as discussed in the previous subsection that enables sensors to detect the targets. For instance, the presence of multiple targets extends the detection range of the sensor due to the superposition of the target energy. As discussed, it is the superposition of power property that allows one to estimate the number of targets. For the disc model, the number of targets is always ambiguous. Consider a proximity sensor network with one cluster of detections. The cluster could be the result of one target or hundreds of targets within the same vicinity. Beyond the fact that the disc model is an idealized representation of the behavior of the sensor, the inability of the disc sensing model to disambiguate the number of targets is a severe weakness that can affect the performance of tracking algorithms based on this model as demonstrated in Section IV.

III. Multiple Target Tracking

The multiple target tracking approach for the binary proximity sensor network proposed in this paper exploits the theory of finite point processes (or random finite set statistics (FISST)). Rigorous derivations of multiple target tracking from FISST can be found in [11], [13], [18]. In essence, at a given snapshot in time, the set of all targets is modeled as a realization of a finite point process. The tracking approach simply updates statistics about the posterior distribution of the finite point process given the sensor measurements.

A. Finite Point Process Basics

For the purposes of this paper, a finite point process is a random process whose realization is a set of points within a d-dimensional state space $\mathbb{R}^d$. The realization can be viewed as a sample from a two step process where the number of objects n is sampled from the probability mass function (pmf) $f_n(n)$, and then the n d-dimensional states are sampled from the joint probability density function (pdf) $f_{x|n}(\mathbf{x}_1, \ldots, \mathbf{x}_n|n)$ that is conditioned on the number of targets. The overall state of a realization of a finite point process is the number of points and the individual state vectors describing each point. Thus, the finite point process state is a variable dimension state

$\mathcal{X} = \begin{bmatrix} n_{\mathcal{X}} & \mathbf{x}_1^T & \dots & \mathbf{x}_{n_{\mathcal{X}}}^T \end{bmatrix}^T$ of size $(n_{\mathcal{X}} d + 1) \times 1$. The probability density for the finite point process state is[1]

$$f(\mathcal{X}) = f(n_{\mathcal{X}}; \mathbf{x}_1, \dots, \mathbf{x}_{n_{\mathcal{X}}}) = f_{x|n}(\mathbf{x}_1, \dots, \mathbf{x}_{n_{\mathcal{X}}} | n_{\mathcal{X}}) f_n(n_{\mathcal{X}}), \quad (6)$$

which is referred to as the multiobject density function for the finite point process. As any probability density, the integral over all possible realizations is one. Given that the number of arguments within the density differs based on the number of realized points, the integration of all realizations is

$$\int f(\mathcal{X}) \delta\mathcal{X} = \sum_{n_{\mathcal{X}}=0}^{\infty} \int f(n_{\mathcal{X}}; \mathbf{x}_1, \dots, \mathbf{x}_{n_{\mathcal{X}}}) d\mathbf{x}_1 \cdots d\mathbf{x}_{n_{\mathcal{X}}} = \sum_{n_{\mathcal{X}}=0}^{\infty} f_n(n_{\mathcal{X}}) = 1. \quad (7)$$

A useful statistics to summarize the multiobject density is the probability hypothesis density (PHD), which represents the support of the density for a particular target state over all possible target count hypotheses, i.e.,

$$D(\mathbf{x}) = \sum_{n_{\mathcal{Y}}=1}^{\infty} \int \left(\sum_{i=1}^{n_{\mathcal{Y}}} \delta(\mathbf{y}_i - \mathbf{x}) \right) f(n_{\mathcal{Y}}; \mathbf{y}_1, \dots, \mathbf{y}_{n_{\mathcal{Y}}}) d\mathbf{y}_1 \cdots d\mathbf{y}_{n_{\mathcal{Y}}} \quad (8)$$

Therefore, the PHD represents the density of the expected number of objects at a particular target state $\mathbf{x}$; that is, the integral of the PHD in the target space represents the expected number of objects. In short, the PHD filter not only provides the density of multiple targets but also the estimates of the number of targets in the scene.

B. Track Filtering

Single target track filtering basically transforms a posterior target density for time $t-1$ into a predicted (or prior) density for time t through the use of a stochastic target motion model. Then the prior density is transformed to a posterior density through Bayes' rule in the likelihood (or measurement) update stage. Similarly, it is possible to perform multiple target track filtering using the multiobject density. A particle implementation of such a Bayes multitarget filter is presented in [13]. The main problem with the Bayes multitarget filter is that the dimensionality of the multiobject density function is not bounded, and as the number of targets increases, the support of the multiobject density migrates to portions of the density representing increasingly higher dimensionality.

The probability hypothesis density (PHD) filter was introduced by in [11] as a means to control the curse of dimensionality. Instead of tracking the full multiobject distribution over time for the finite point process, the filter simply tracks the PHD as defined in (8), which is a first order moment of the distribution. Just like any other track filter, the PHD filter is composed of a prediction and a likelihood update stage. The prediction step starts with the PHD $D_{t-1|t-1}(\mathbf{x})$ of the prior multiobject density, i.e., the density of the finite point process given measurement up to time $t-1$. We refer to $D_{t-1|t-1}(\mathbf{x})$ as the prior PHD. The prediction step determines the PHD $D_{t|t-1}(\mathbf{x})$ for the density of the finite point process as it evolves to time t. We refer to $D_{t|t-1}(\mathbf{x})$ as the predicted PHD. The evolution considers target motion, death, and birth models for the points. In [11], Mahler proved a simple relationship between the prior and predicted PHDs (see (75) in [11]). This work does not consider the target death and birth models, and without these models, the relationship simplifies to

$$D_{t|t-1}(\mathbf{x}) = \int f_{t|t-1}(\mathbf{x}|\mathbf{w}) D_{t-1|t-1}(\mathbf{w}) d\mathbf{w}, \quad (9)$$

where $f_{t|t-1}(\mathbf{x}|\mathbf{w})$ is the density of a point's state $\mathbf{x}$ at time t conditioned on its state $\mathbf{w}$ at time $t-1$. The specific form for $f_{t|t-1}(\mathbf{x}|\mathbf{w})$ represents the motion model. The motion model evokes a Markov assumption for the movement of points, and it assumes targets move independently of each other.

The likelihood update stage evokes Bayes' rule to determine the PHD of the posterior multiobject density given the measurements up to time t. In general, the resulting PHD $D_{t|t}(\mathbf{x})$, which we refer to as the posterior PHD, cannot be uniquely determined solely by the predicted PHD. In other words, two mutiobject density functions that have the same PHD will not in general have the same PHD after the likelihood update. To ground the density, the PHD filter approximates the predicted multiobject density with the density of a Poisson point process (PPP). As show in Theorem 4 in [11], the best Poisson approximation in the sense of the Kullback-Leibler divergence is the Poisson point process whose intensity function is the predicted PHD, i.e.,

$$f_{t|t-1}(\mathcal{X}) = f_{t|t-1}(n; \mathbf{x}_1, \dots, \mathbf{x}_n) = \frac{1}{n!} \left(\prod_{i=1}^{n} D_{t|t-1}(\mathbf{x}_i) \right) \exp\left\{ - \int D_{t|} \right. \quad (10)$$

Given the density of the measurements conditioned on the realization of the point process, Bayes' rule leads to the posterior multiobject density

$$f_{t|t}(n; \mathbf{x}_1, \dots, \mathbf{x}_n) = \frac{1}{C} f_{Z|X}(\mathbf{z}|\mathcal{X}) \frac{1}{n!} \left(\prod_{i=1}^{n} D_{t|t-1}(\mathbf{x}_i) \right) \exp\left\{ - \int D_{t|t-} \right. \quad (11)$$

where C is the constant so that the posterior integrates to one, i.e.,

$$C = \sum_{n=0}^{\infty} \int f_{Z|X}(\mathbf{z}|\mathcal{X}) \frac{1}{n!} \left(\prod_{i=1}^{n} D_{t|t-1}(\mathbf{x}_i) \right) \exp\left\{ - \int D_{t|t-1}(\mathbf{x}) d\mathbf{x} \right\} d\mathbf{x} \quad (12)$$

Then, the posterior PHD $D_{t|t}(\mathbf{x})$ is calculated by applying (8) over (11). Finally, $D_{t|t}(\mathbf{x})$ is treated as the PHD for the prior multiobject density for the next round of prediction and measurement updates.

In the traditional use of the PHD as proposed by Mahler, the measurements are modeled as a point process whose points are

[1] As defined, $f(\mathcal{X})$ is virtually the same as $\frac{1}{n!} j_n(\{\mathbf{x}_1, \dots, \mathbf{x}_n\})$ where $j_n(\cdot)$ is the Janossy density [11]. For the sake of notational convenience in the development of the particle filter, the symmetry property of the Janossy density is not maintained in $f(\mathcal{X})$, e.g., the density (21) is technically not symmetric. Forcing the multiobject density to be symmetric in the particle filter development is straightforward but requires additional computational resources, e.g., memory, and arrives at the same PHD due to collapsing the density (see (23)) and the symmetry of the likelihood given by (13).

a mixture of a clutter PPP and points spawned by targets. In this case, $f_{Z|X}$ is a multiobject density function conditioned on the realization of the target process. Furthermore, an analytical relationship exists between the posterior and predicted PHDs so that the use of Bayes' rule over the PPP approximation for the multiobject density is implicit.[2] As a result, the particle implementation of the traditional PHD filter only requires particles to represent the PHD. In general, we view the PHD filter as the process of performing the prediction and likelihood updates for the tracking of the PHD of the finite point process conditioned on the observations via (9), (11), and (8). When the measurements are a mixture of a clutter PPP and target spawned measurements, then the PHD filter is the familiar implementation.

For the application of multiple target targeting using binary sensor measurements over a 2-D field, the target state is a 4-D vector representing the 2-D position $\mathbf{y}$ and 2-D velocity $\mathbf{v}$ of the target, i.e., $\mathbf{x} = \begin{bmatrix} \mathbf{y}^T & \mathbf{v}^T \end{bmatrix}^T$ and $d = 4$. The discretized continuous-time white noise acceleration (DCWNA) model is employed for the motion model [23]. Each binary sensor measurement has a pmf given by (4) or (5) for the probabilistic or disc model, respectively. The measurement model also assumes the sensor measurements are statistically independent. For a proximity sensor network of N_s sensors, the likelihood $f_{Z|X}$ for measurements $\mathbf{z} \in \{0,1\}^{N_s}$ is given by

$$f_{Z|X}(\mathbf{z}|\mathcal{X}) = \prod_{m=1}^{N_s} P_d(\mathbf{s}_m, \mathcal{Y})^{z_m} \left(1 - P_d(\mathbf{s}_m, \mathcal{Y})\right)^{1-z_m}, \tag{13}$$

where $\mathcal{Y} = [\mathbf{y}_1, \ldots, \mathbf{y}_n]$ is extracted from $\mathcal{X}$, $\mathbf{s}_i$ is the location of the i-th sensor, and $\mathbf{z}$ is the collection of binary measurements at the current time. Note that the likelihood is a pmf evaluated at the values of the reported sensor measurements. From (4) (or (5)) and (13), it is clear that the likelihood is symmetric with respect to any permutation of the target state indices within $\mathcal{X}$. To the best of our knowledge, the calculation of the posterior PHD from the posterior multiobject density after the likelihood update does not simplify as a simple analytical transformation of the prior PHD.

C. Particle PHD Filter for Binary Sensors

Unlike the particle implementation of the traditional PHD filter, the particle implementation of the general PHD filter requires particles to sample the PHD, and other particle derived from the PHD particles to sample the predicted multiobject density. The basic steps of the proposed particle PHD filter are to 1) propagate the PHD particles via prediction update in (9), 2) sample the predicted multiobject density from the PPP approximation in (10) to form multiobject density particles, 3) compute the likelihood update in (11) using the multiobject density particles as an approximation of the actual density, and 4) collapse the multiobject density particles into PHD particles through (8). This section explains how to perform these steps.

To begin, the prior PHD at time $t-1$ is approximated by P single target particles $\{w_{t-1}^{(p)}, \mathbf{x}_{t-1}^{(p)}\}_{p=1}^{P}$ so that

$$D_{t-1|t-1}(\mathbf{x}) \approx \sum_{p=1}^{P} w_{t-1}^{(p)} \delta(\mathbf{x} - \mathbf{x}_{t-1}^{(p)}), \tag{14}$$

where $\delta(\cdot)$ is the Dirac delta function. Then, the estimated number of targets is the integral of the PHD so that

$$\hat{N}_{t-1} \approx \sum_{p=1}^{P} w_{t-1}^{(p)}. \tag{15}$$

To compute the predicted PHD, the p-th particle is sampled from the proposal density $x_t^{*(p)} \sim f_{t|t-1}(\mathbf{x}|\mathbf{x}_{t-1}^{(p)})$. Given the DCWNA motion model, the predicted particles are obtained by diffusing the prior particle such that

$$\mathbf{x}_t^{*(p)} = F\mathbf{x}_{t-1}^{(p)} + Q^{\frac{1}{2}}\mathbf{v}^{(p)}, \tag{16}$$

where $\mathbf{v}^{(p)}$ is sampled from a white Gaussian random number generator, and F and Q are the state transition and process noise covariance matrices, respectively (see [23]). In other words, the proposal density is Gaussian with mean $F\mathbf{x}_{t-1}^{(p)}$ and covariance Q. Since the proposal density matches the actual motion model, the predicted PHD is simply

$$D_{t|t-1}(\mathbf{x}) \approx \sum_{p=1}^{P} w_{t-1}^{(p)} \delta(\mathbf{x} - \mathbf{x}_t^{*(p)}). \tag{17}$$

Note that since the target prediction step does not incorporate a target birth and death model, the predicted PHD still integrates to $\hat{N}_{t-1}$.

To perform the likelihood update, samples from the PPP approximation of the predicted multiobject density given by (10) must be generated where the predicted PHD is (17). The two stage PPP sampling approach as explained in [24] is employed. For the p-th multiobject particle, the number of hypothesized targets is sampled from a Poisson distribution with mean $\hat{N}_{t-1}$, that is, $n^{(p)} \sim Poisson(\hat{N}_{t-1})$. Then, each of the states of the $n^{(p)}$ targets is sampled from the normalized predicted PHD given by (17) divided by $\hat{N}_{t-1}$.[3] This is equivalent to selecting each of the target states to be one of the P PHD particles where the particle to select is sampled from the multinomial distribution given by $\frac{w_{t-1}^{(p)}}{\hat{N}_{t-1}}$ for $p = 1, \ldots, P$. The proposed method uses this PPP sampling approach to generate Pn_{ex} multiobject particles where $n_{ex} \geq 1$ is a user supplied parameter.

When a modest number of particles are used to approximate the predicted PHD, it is possible for the particles to drift away from the true target locations due to an imperfect motion model. To regularize the process, it is helpful to generate some innovative multiobject particles by sampling from likely target locations given the current set of measurements. For these particles, the number of targets represented by a single multiobject particle is still sampled from a Poisson distribution with mean $\hat{N}_{t-1}$. The target states are generated from a proposal density $q(\cdot|\mathbf{z})$ that is conditioned on the current measurements.

[2] [11] uses probability generating functionals to derive the PHD likelihood update equation where the usage of Bayes' rule via (11) is also implicit.

[3] Normalized to integrate to one.

This proposal density could be the scaled likelihood using the Metropolis-Hastings method [25], but such a method is of high computational complexity. In this paper, the proposal density for the position components of the target states is a rectangular bounding box that encompasses all sensors that report detections. The velocity components of the target states are set to zero. The bounding box represents a computationally efficient proposal density that approximates the more costly method of incorporating the feasible target area (FTA) used in [20], [21].

Overall, J innovative multiobject particles are generated, and $P_{ex} = Pn_{ex} + J$ multitarget particles represent the predicted target density

$$f_{t|t-1}(\mathcal{X}) \approx \sum_{p=1}^{P_{ex}} \tilde{\delta}(\mathcal{X}; \mathcal{X}_t^{(p)}), \tag{18}$$

where

$$\tilde{\delta}(\mathcal{X}; \mathcal{X}_t^{(p)}) = \begin{cases} 0 & \text{if } |\mathcal{X}| \neq |\mathcal{X}_t^{(p)}| \\ \prod_{i=1}^{n_t^{(p)}} \delta(\mathbf{x} - \mathbf{x}_{t,i}^{(p)}) & \text{otherwise} \end{cases}$$

is the equivalent of a delta function centered at $\mathcal{X}_t^{(p)}$ over the multiobject space, and $n_t^{(p)}$ and $x_{t,i}^{(p)}$ are extracted from $\mathcal{X}_t^{(p)}$. It is not difficult to verify that $\tilde{\delta}(\cdot)$ satisfies the sampling property

$$\int f(\mathcal{X})\tilde{\delta}(\mathcal{X}; \mathcal{X}_t^{(p)})\delta\mathcal{X} = f(\mathcal{X}_t^{(p)}) \tag{19}$$

so that

$$f(\mathcal{X})\tilde{\delta}(\mathcal{X}; \mathcal{X}_t^{(p)}) = f(\mathcal{X}_t^{(p)})\tilde{\delta}(\mathcal{X}; \mathcal{X}_t^{(p)}). \tag{20}$$

Also, the weights are not explicit in (18) since they are equal to one due to the fact the particles are sampled from the desired density. In effect, the generation process creates particles sampled from a PPP with an intensity (or PHD) of

$$D(\mathbf{x}) = \frac{Pn_{ex}}{P_{ex}} D_{t|t-1}(\mathbf{x}) + \frac{J}{P_{ex}} D_r(\mathbf{x}),$$

where $D_r(\mathbf{x})$ represents the portion of the regulated PHD due to the innovative particles. It is uniform over the bounding box surrounding the sensors reporting detections, and it integrates out to $\hat{N}_{t-1}$ so that the estimated number of targets due to regularization does not change. The ratio J over P_{ex} represents the importance the regularization places over on current measurements relative to the prior measurements. When $J = 0$, the predicted distribution is the normal predicted distribution. On the other hand, when $J = P_{ex}$ the predicted distribution completely ignores the prior measurements. A moderate value of J prevents the set of particles to lose track of the target due 1) to either too few particles to properly represent the density or 2) to an overly simplistic dynamical model.

The likelihood update passes the density given by (18) through (11) and (12) using the likelihood given by (13). As a result of the sampling property (19)-(20), the posterior density is

$$f_{t|t}(\mathcal{X}) \approx \sum_{p=1}^{P_{ex}} w_p^f \tilde{\delta}(\mathcal{X}; \mathcal{X}_t^{(p)}), \tag{21}$$

where the weights

$$w_p^f = \frac{1}{C} f_{Z|X}(\mathbf{z}_t | \mathcal{X}_t^{(p)}), \tag{22}$$

$\mathbf{z}_t$ are the binary measurements collected at time t, and C is a constant so that the weights sum to one.

The final step of the PHD filter is to collapse the posterior density back down to the posterior PHD by inserting (21) into (8). As a result,

$$\begin{aligned} D_{t|t}(\mathbf{x}) &\approx \sum_{p=1}^{P_{ex}} w_p^f \sum_{i=1}^{n^{(p)}} \delta(\mathbf{x} - \mathbf{x}_{t,i}^{(p)}), \\ &\approx \sum_{p=1}^{P^*} w_t^{*(p)} \delta(\mathbf{x} - \mathbf{x}_t^{*(p)}), \end{aligned} \tag{23}$$

where $P^* = \sum_{p=1}^{P_{ex}} n^{(p)}$, and there is a one-to-one correspondence between the PHD particles $\mathbf{x}_t^{*(p)}$ and multiobject particle components $\mathbf{x}_{t,i}^{(p)}$. Each multiobject particle component leads to a PHD particle, and when the k-th PHD particle originated from the l-th component of the m-th multiobject particle, then $\mathbf{x}_t^{*(k)} = \mathbf{x}_{t,l}^{(m)}$ and $w_t^{*(k)} = w_m^f$. The expression for the conversion of multiobject particles to PHD particles has appeared in [13] (see Section 2E) for generating target state estimates in implementation of the Bayes multitarget filter. Integration of (23) leads to a target count estimate of $\hat{N}_t = \sum_{p=1}^{P_{ex}} n^{(p)} w_p^f = \sum_{p=1}^{P^*} w_k^{*(p)}$. Finally, the PHD is resampled down to P particles so that the number of samples does not continue to grow after each likelihood update. To this end, the P particles are selected from the P_{ex} particle using sampling with replacement from the multinomial distribution $\frac{w_t^{*(p)}}{\hat{N}_t}$. After this final resampling stage,

$$D_{t|t}(\mathbf{x}) \approx \sum_{p=1}^{P} w_t^{(p)} \delta(\mathbf{x} - \mathbf{x}_t^{(p)}), \tag{24}$$

where $w_t^{(p)} = \hat{N}_t / P$. For the next stage of prediction and measurement updates, (24) replaces (14) as the prior PHD.

The implementation of the PHD particle filter at any time is summarized in Fig. 2: Start with the prior PHD particles (Step 1), form the predicted PHD particles via the target motion model (Step 2), expand to the particle representation of the PPP multiobject density (Steps 3-5), perform the measurement (or likelihood) update (Step 6), and calculate the posterior PHD (Step 7-10). After the P particles for $D_{t|t}(\mathbf{x})$ are obtained, the k-means method is used to group the particles into $\texttt{round}(\hat{N}_t)$ clusters. The centroids of these clusters are used as the estimated target states.

The particle implementation of the PHD filter in Fig. 2 is able to estimate the number of targets without any target birth and death model due to the expansion of the PHD particles to multiobject particles. Specifically, Step 3 means that the PHD does explore hypotheses of various numbers of targets. Then, the likelihood update is able to emphasize hypotheses whose target counts better explain the measurements $\mathbf{z}$ at the given snapshot in time. It is these hypotheses that mostly determine

1) Given P prior PHD particles $\{w_{t-1}^{(k)}, \mathbf{x}_{t-1}^{(k)}\}_{k=1}^{P}$ where $\hat{N}_{t-1} = \sum_{p=1}^{P} w_{t-1}^{(p)}$.
2) Obtain P predicted PHD particles: $\mathbf{x}_t^{*(p)} = F\mathbf{x}_{t-1}^{(p)} + Q^{\frac{1}{2}}\mathbf{v}^{(p)}, p = 1, 2, \ldots, P$, where $\mathbf{v}^{(p)}$ is a zero mean white Gaussian noise vector.
3) Obtain P_{ex} Poisson samples with mean $\hat{N}_{t-1}$: $n^{(k)} \sim Poisson(\hat{N}_{t-1}), k = 1, 2, \ldots, P_{ex}$, where $P_{ex} = Pn_{ex} + J$.
4) Obtain Pn_{ex} predicted multiobject particles $\{\mathbf{x}_{t,1}^{(k)}, \ldots, \mathbf{x}_{t,n^{(k)}}^{(k)}\}_{k=1}^{Pn_{ex}}$ where the k-th multiobject particle consists of $n^{(k)}$ target states drawn (with replacement) from $\{\mathbf{x}_t^{*(p)}\}_{p=1}^{P}$ with probability $\frac{w_{t-1}^{(p)}}{\hat{N}_{t-1}}$.
5) Obtain J innovative multiobject particles $\{\mathbf{x}_{t,1}^{(k)}, \ldots, \mathbf{x}_{t,n^{(k)}}^{(k)}\}_{k=Pn_{ex}+1}^{Pn_{ex}+J}$ where the k-th multiobject particle consists of $n^{(k)}$ target state samples drawn uniformly from a rectangular box that bounds all the detecting sensors.
6) Obtain the weights $\{w_k^f\}_{k=1}^{P_{ex}}$ for the P_{ex} multiobject particles $\{\mathbf{x}_{t,1}^{(k)}, \ldots, \mathbf{x}_{t,n^{(k)}}^{(k)}\}_{k=1}^{P_{ex}}$ by (13), and then normalize the weights to sum to one.
7) Convert P_{ex} multiobject particles to P^* PHD particles at time t by (21) to form $\{w_t^{*(k)}, x_t^{*(k)}\}_{k=1}^{P^*}$.
8) Estimate the number of objects at time t: $\hat{N}_t = \sum_{k=1}^{P_{ex}} n^{(k)} w_k^f$.
9) Obtain P posterior PHD particles drawn (with replacement) from $\{\mathbf{x}_t^{*(p)}\}_{p=1}^{P^*}$ with probability $\frac{w_t^{*(p)}}{\hat{N}_t}$.
10) Weigh each PHD particle $\mathbf{x}_t^{(p)}$ uniformly as $w_t^{(p)} = \hat{N}_t/P$.
11) Let $t := t + 1$ and goto Step #1.

Fig. 2. Steps of the particle implementation of the PHD filter for proximity sensor networks.

the posterior PHD particles. Nevertheless, the particle implementation could be enhanced by explicit target birth and death models. This is left for future investigation.

D. Initialization

The PHD filter begins with an initial set of particles at time $t = 0$ to approximate $D_{0|0}(\mathbf{x})$. For most of the simulations in Section IV, we generated P particles where the location states are uniformly sampled over the surveillance region covered by the sensors, and the velocity states are sampled from a Gaussian with mean zero and $\sigma = 10$. The weight associated to each particle is initially set to N/P where N is a prior estimate of the number of targets. In the simulations, N is set up to be 0.5 for the PHD filter. [4] For the clairvoyant particle filters in Section III-E and Section III-F, N is the true number of targets because we assume the number of targets is known *a priori*. To determine the sensitivity of the PHD to the initialization, some of the simulations generated the location states by restricting these values to be drawn uniformly within the rectangular bounding box for sensors reporting detections.

E. Clairvoyant multitarget particle filter

Unlike the PHD filter, the particle implementation of multitarget Bayes filter requires explicit target birth and death models. For example, when the scene contains N targets, the multiobject particles that survive will correspond to N targets. Without explicit birth and death models, when more targets emerge or if targets leave the scene, there is no mechanism for multiobject particles corresponding to target counts different than N to emerge. To perform a comparison of the PHD filter with the multitarget particle filter in this paper where birth/death models are not considered, a clairvoyant multiobject particle filter is used. This allows one to understand the effectiveness of the PHD filter to track multiple targets. The particle filter is clairvoyant in the sense that the number of targets N is known *a priori*. Therefore, no target birth/death model is needed. The performance of the filter indicates the effectiveness of standard processing when the number of targets need not be estimated. Effectively, the N-target clairvoyant particle filter (CPF) is a particle filter implementation of the multitarget sequential Bayesian filter when the multiobject density function $f(n_{\mathcal{X}}; \mathbf{x}_1, \ldots, \mathbf{x}_{n_{\mathcal{X}}})$ has nonzero support only for $n_{\mathcal{X}} = N$. Thus, the p-th multiobject particle is $\mathcal{X}_t^{(p)} = \left[\begin{array}{cccc} N & \mathbf{x}_{t,1}^{(p)^T} & \ldots & \mathbf{x}_{t,N}^{(p)^T} \end{array} \right]^T$.

Initially at time $t = 0$, P multiobject particles are generated. These particles are composed of N 4-state subparticles that collectively form a sampling of $f_{0|0}(N; \mathbf{x}_1, \ldots, \mathbf{x}_N)$. For cases where targets appear or disappear at certain times, the multiobject density function is adjusted accordingly. Given P multiobject particles, the evolution of the particles $\{\mathcal{X}_{t-1}^{(p)}\}_{p=1}^{P}$ at time $t - 1$ proceeds as follows:

1) Obtain P predicted multiobject particles: $\mathcal{X}_t^{(p)} = \{\mathbf{x}_{t,i}^{(p)}\}_{i=1}^{N}$ where $\mathbf{x}_{t,i}^{(p)} = F\mathbf{x}_{t-1,i}^{(p)} + Q^{\frac{1}{2}}\mathbf{v}^{(p)}, p = 1, 2, \ldots, P$.
2) Obtain J innovative multiobject particles $\mathcal{X}_t^{(p)} = \{\mathbf{x}_{t,i}^{(p)}\}_{i=1}^{N}$ where the p-th multiobject particle consists of N target states drawn uniformly from a rectangular box that bounds all the detecting sensors.
3) Obtain the weights $\{w_p^f\}_{p=1}^{P+J}$ for the $P + J$ multiobject

[4] This is to show that despite the mismatch in the initialization, the target count can quickly converge to the true value.

particles $\{\mathcal{X}_t^{(p)}\}_{p=1}^{P+J}$ where the weight for the p-th multiobject particle w_p^f is computed by (13).

4) Resample the $P+J$ multiobject particles to obtain P particles $\{\mathcal{X}_t^{(p)}\}_{p=1}^{P}$ where $\mathcal{X}_t^{(p)}$ is selected with probability $\frac{w_p^f}{N}$.
5) Let t:=t+1 and goto Step #1.

The components (target state vectors) in the multiobject particles may not align between particles. In other words, the i-th target component in the particle $\mathcal{X}_t^{(m)}$ and the i-th target component in the particle $\mathcal{X}_t^{(n)}$ when $m \neq n$ may not correspond to the same target. To calculate a minimum mean squared error (MMSE) estimate of the target states, the subparticles in each particle are assigned ground truth targets by solving the 2-D assignment problem [26]. That is each subparticle is matched to one and only one ground truth target and vice versa. Finally, the weighted average of all subparticles associated to a particular ground truth target is computed as the state estimate for that target. Clearly, the CPF is incorporating information that is unknown to the filter to provide the state estimates. The purpose of the CPF is to simply baseline the performance of the PHD method.

F. Clairvoyant PHD

In the CPF, the grouping of subparticles into particles affects tracking performance because this grouping is always maintained in the filter. On the other hand, the PHD continues to mix up target state particles when it forms the multiobject density from the PHD. This process allows for innovative combinations of single-target particles. In some sense, the PHD filter performs a crossover step similar to genetic programming. However, the PHD is also estimating N, which the CPF does not have to do. To determine the effectiveness of these crossover operations without the burden of estimating N, we also consider a modified PHD where N is known. Specifically, Step #3 of the PHD filter in Fig. 2 is changed so that $n^{(k)} = N$ for $k = 1, \ldots, P_{ex}$. We refer to this PHD as the clairvoyant PHD.

G. Performance Measures

The Wasserstein [27] and optimal subpattern assignment (OSPA) [28] metrics are common measures of performance for PHD track filters. They combine the effects of position and cardinality errors in a single quantity. However, we wish to deconflict these two types of errors. The cardinality error is simply $|\hat{N}_t - N_t|$ where $\hat{N}_t$ and N_t are the estimated and actual number of targets in the scene, respectively.

For the target state errors, we modify the OPSA metric [28] to consider only the position errors and not the cardinality errors. This performance measure operates on the set of estimated target states X and the set of ground truth target states Y representing the position components. We refer to the modified performance measure as the *cardinality agnostic OPSA* (CA-OPSA). The CA-OPSA is not a metric in the strict sense as a measure of zero does not imply $X = Y$ due to possible differences in the sizes of sets X and Y. Formally, the CA-OPSA is

$$\begin{aligned} D(X,Y) &= \min \frac{1}{S} \sum_{i=1}^{|X|} \sum_{j=1}^{|Y|} C_{i,j} d(x_i, y_j), \qquad (25) \\ \text{s.t.} \quad & \textstyle\sum_{i=1}^{|X|} C_{ij} \leq 1, \sum_{j=1}^{|Y|} C_{ij} \leq 1, \\ & \sum_{i=1}^{|X|} \sum_{j=1}^{|Y|} C_{ij} = S, \\ & S = \min(|X|, |Y|), \text{ and } C_{ij} \in \{0,1\}, \end{aligned}$$

where $d(x_i, y_j)$ is a user selected distance measure between the i-th and j-th position states for sets X and Y, respectively. In this paper, $d(\cdot,\cdot)$ is the standard ℓ^2 norm. In essence, the CA-OPSA represents the average root mean squared (RMS) error for the 2-D assignment of the estimated and ground truth target states such that one and only one estimate is assigned to a ground truth element and vice versa. If $|X| > |Y|$, the extra target estimates are not assigned to ground truth elements. Likewise, if $|X| < |Y|$, the extra ground truth elements are not assigned to target estimates. Note that other metrics do exist that are relatively insensitive to differences in the target cardinality, e.g., the Hausdorff distance [27]. For the sake of simplicity, this paper only considers the CA-OSPA to characterize the localization performance of the proposed PHD filter.

IV. Simulations

A. Mode Matching/Mismatching Cases

The first set of simulations considers four scenarios where targets move through a surveillance region of size 1km $\times$ 1km for 100 or 300 seconds. Filter updates occur in snapshot intervals of one second. The geometry of Scenario A is illustrated in Fig. 3. In this scenario, two targets travel at a constant velocity with a speed of about 10m/s. The two targets cross paths at $t = 50$s. Fig. 4 provides the geometry for Scenario B. In this scenario, two targets are maneuvering. The two targets never cross paths, but they do converge and diverge with a closest approach occurring around $t = 37$s. Fig. 5 illustrates Scenario C where three targets move in and out of the surveillance region during the 100 seconds. Finally, Fig. 6 illustrates Scenario D where five targets move in and out of the surveillance region during the 300 seconds. The lower number at an end of a track represents the starting time of the track. Likewise, the larger number represents the end time of the track. For example, the first track starts at $t = 1$ and ends at $t = 300$, the second starts at $t = 31$ and ends at $t = 270$, and the third starts at $t = 61$ and ends at $t = 210$, etc. As a result, the number of targets varies from 1 to 5 at any given time.

We believe that the probabilistic sensing model provides a more realistic representation than the disc model for the behavior of a proximity sensor to its environment. However, we are interested in understanding the robustness of multi-target tracking when considering either model. Therefore, the simulations consider both models for actual sensing behavior and for insertion into the tracker. Overall, there are four cases. The first two are matching cases: 1) the actual sensing model

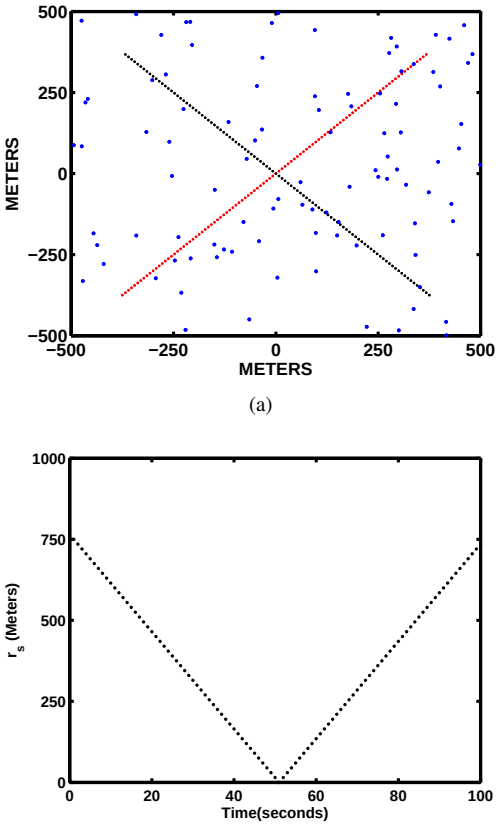

Fig. 3. Scenario A: (a) Geometry of a 100-sensor network with two targets traveling at constant velocities, and (b) separation distance between the two targets vs. time.

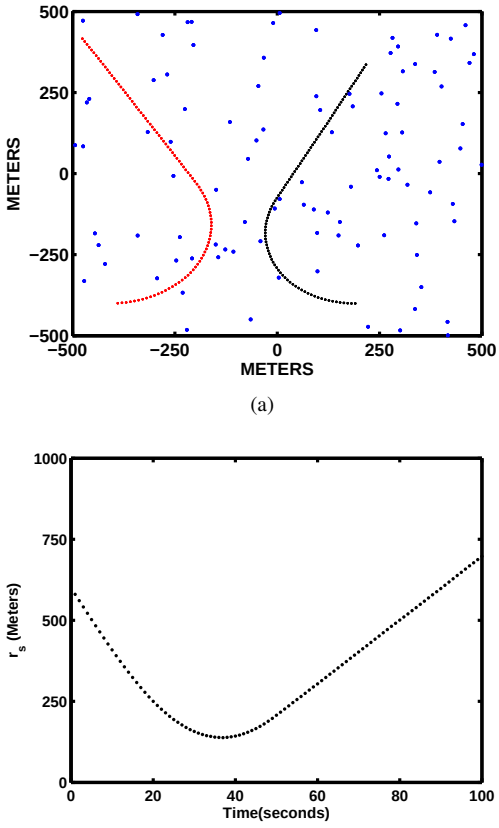

Fig. 4. Scenario B: (a) Geometry of a 100-sensor network with two targets maneuvering, and (b) separation distance between the two targets vs. time.

is the probabilistic model and the filter assumes the same probabilistic model, and 2) the actual sensing model is the disc model and the filter assumes the same disc model. The final two are mismatching cases: 3) the actual sensing model is the probabilistic model but the filter assumes the disc model, and 4) the actual sensing model is the disc model but the filter assumes the probabilistic model.

For the probabilistic sensing model, the threshold is set so that $P_{fa} = 0.001$. In the disc model, $r_{eff} = 117$m, which is the distance that makes $P_d = 0.5$ for $P_{fa} = 0.001$ in the probabilistic model. The filter parameters are set to be $P = 1000$, $n_{ex} = 1$, and $J = 100$ so that $P_{ex} = 1100$. For each of the four scenarios, we generated 10 random configurations of 100 proximity sensors, and for each configuration, we ran 10 Monte Carlo realizations of sensor reports. Overall, each scenario consists of 100 simulations. The reported cardinality and RMS position errors (see (25)) for a given snapshot time are averaged over the 100 simulations. For these simulations, we compared the proposed PHD method against the two clairvoyant filters. To the best of our knowledge, no other baseline method exists for proximity sensors that can employ both the probabilistic and disc sending models.

Fig. 7 plots the average RMS position errors versus time for the PHD and two clairvoyant filters for Scenario A over the four sensing model cases. Likewise, Figs. 8- 10 provide

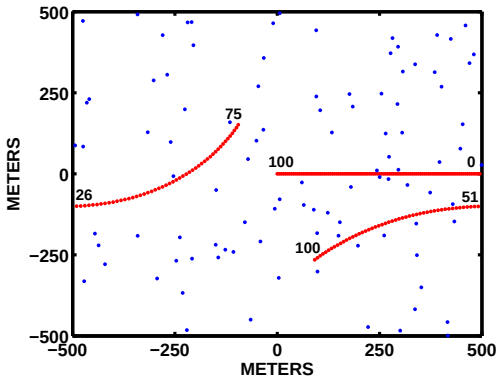

Fig. 5. Scenario C: Geometry of a 100-sensor network with three targets that move in and out of the scene at different times.

similar plots for Scenarios B, C and D, respectively. The relative performances of the PHD compared to clairvoyant filters are consistent over the four scenarios. Regardless of the actual sensing model, the trackers that incorporate the probabilistic model into the measurement likelihood update provide better localization accuracy than those that use the disc model. The probabilistic model accommodates errors in the multiobject particle better than the disc model because perturbations in the particles for the probabilistic model leads to a gradual degradation of the likelihood; whereas, perturba-

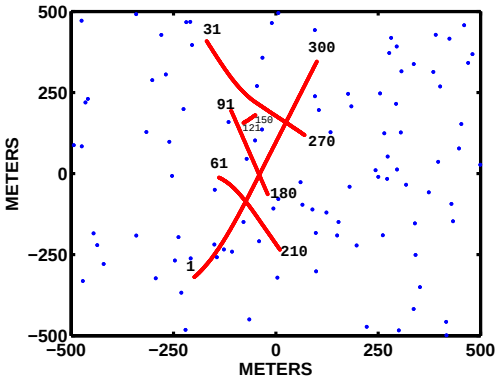

Fig. 6. Scenario D: Geometry of a 100-sensor network with five targets that move in and out of the scene at different times.

tions in the particles can lead to sudden one to zero jumps in the likelihood for the disc model. These properties might explain the better performance by the probabilistic model. When the filters incorporate the probabilistic models (Cases 1 and 4), the filters perform similarly for Scenarios A and B. It takes about 10 seconds for the filters to reach a steady state after initialization, and the localization performance degrades only slightly when the target separation is small. Overall, the localization performances of the filters when implementing the probabilistic model are robust when the actual sensor behavior follows the disc model.

For the matching probabilistic case, the clairvoyant PF is clearly the best, and the clairvoyant PHD is slightly better than the PHD. For Scenario D, the clairvoyant PHD is better than the PHD when the number of targets is small, but comparable when the number of targets is large when tracking is steady. When the filters incorporate the disc model, the performance of the CPF is much poorer; especially for the mismatch case (Case 3). For Case 2, the CPF performance is good when the targets are near each other, and the performance degrades significantly when targets are far apart. This is an artifact of both the proposal function for innovative particles and the lack of the crossover effect that occurs in the PHD implementation. It is possible that the weights for all particles become zero as to be discussed later in Section IV-D. When this happens, all zero weighted particles are then given equal positive weights. As a result, this weighting process then cannot distinguish between particles whose subparticles are closer to the detecting sensors than others. This problem is exacerbated when the sensors actually follow the probabilistic model where false alarms and missed detections can occur. On the other hand, the crossover effect in the PHD makes the probability much smaller that all particles have zero weights. This might explain the improved performance for the PHD methods.

For Scenario C and D, all filters exhibit higher errors when new target appear and disappear in the scene, but the performances of these filters improve when the targets are simply moving. Note the CPF reinitializes when the new targets enter or leave the scene while the PHD filters still propagate the previous particles. The estimation error when the number of targets is large, is higher than that when

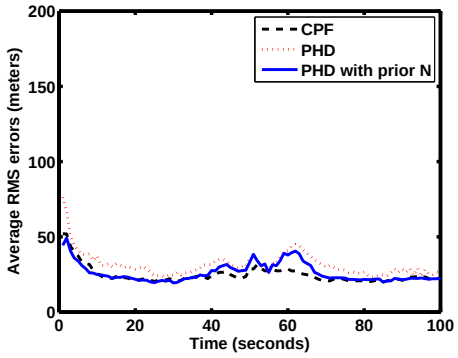

(a)

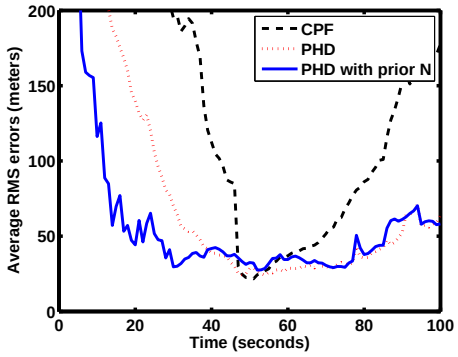

(b)

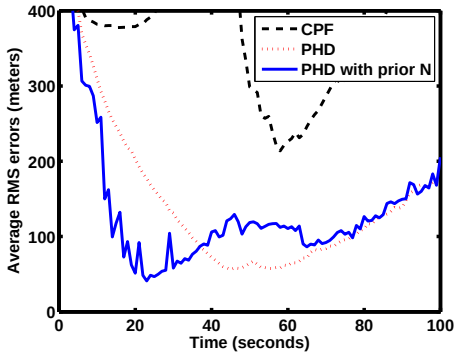

(c)

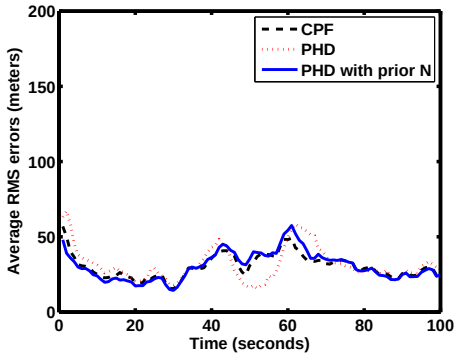

(d)

Fig. 7. Scenario A: CA-OSPA errors for (a) matching probabilistic models, (b) matching disc models, (c) probabilistic sensing model with filter assuming the disc model, and (d) disc sensing model with filter assuming the probabilistic model.

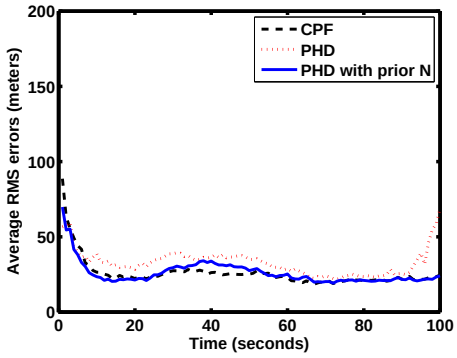

(a)

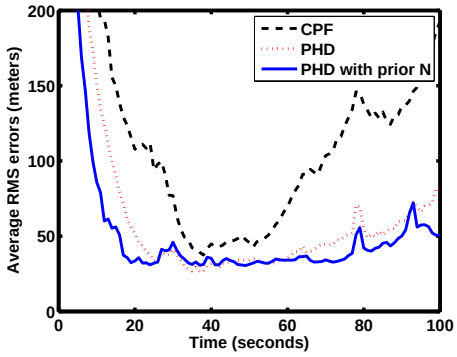

(b)

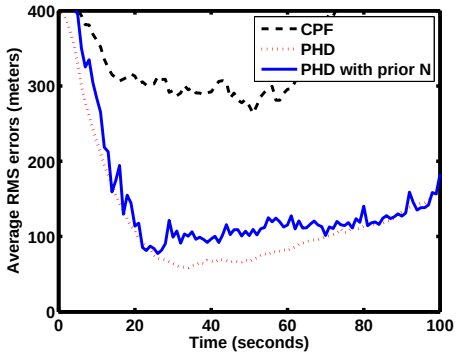

(c)

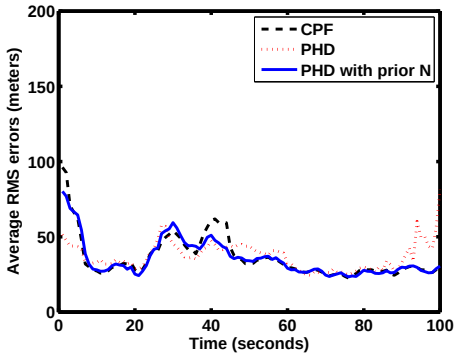

(d)

Fig. 8. Scenario B: CA-OSPA errors for (a) matching probabilistic models, (b) matching disc models, (c) probabilistic sensing model with filter assuming the disc model, and (d) disc sensing model with filter assuming the probabilistic model.

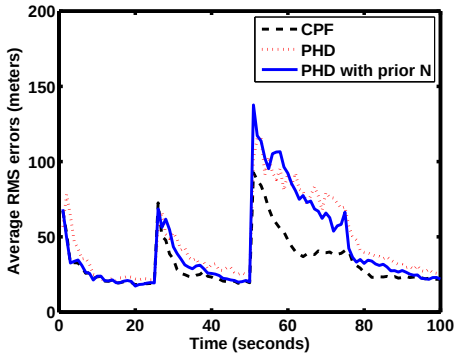

(a)

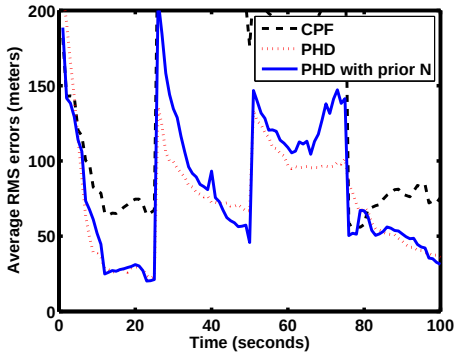

(b)

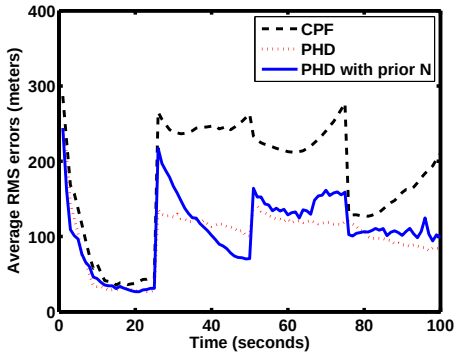

(c)

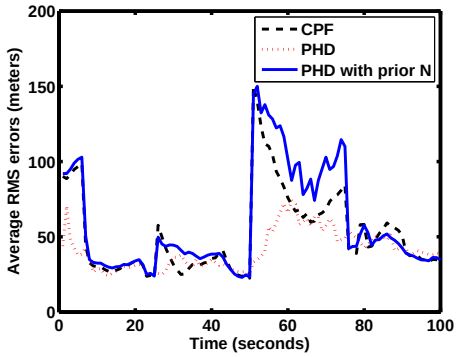

(d)

Fig. 9. Scenario C: CA-OSPA errors for (a) matching probabilistic models, (b) matching disc models, (c) probabilistic sensing model with filter assuming the disc model, and (d) disc sensing model with filter assuming the probabilistic model.

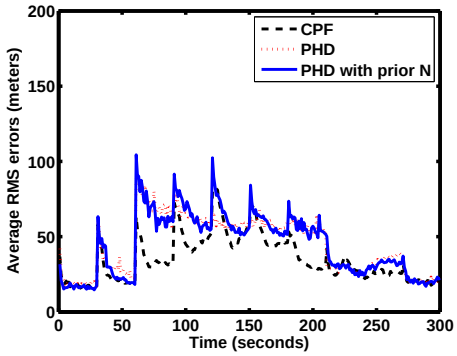

(a)

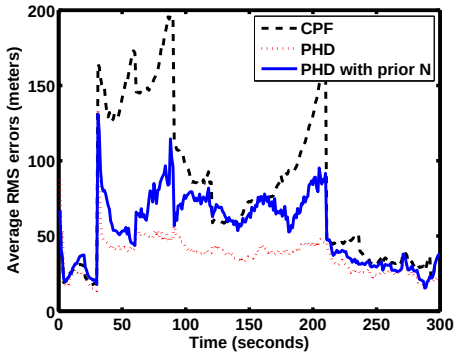

(b)

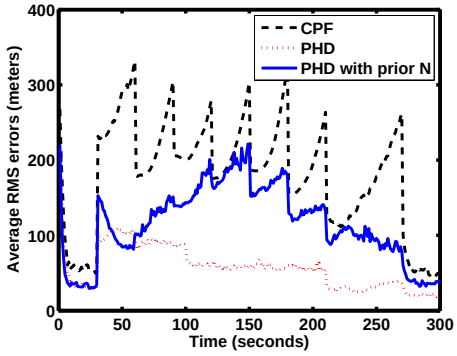

(c)

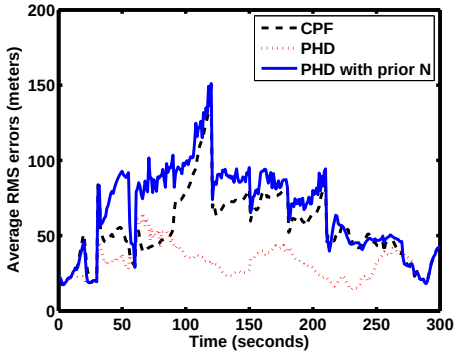

(d)

Fig. 10. Scenario D: CA-OSPA errors for (a) matching probabilistic models, (b) matching disc models, (c) probabilistic sensing model with filter assuming the disc model, and (d) disc sensing model with filter assuming the probabilistic model.

there are fewer targets. In fact, when the number of targets grows to three target or more (Scenarios C and D), the localization error is much poorer than when the number of targets is two or less. The CPF exhibits similar problems in Scenario C and D when employing the disc model as it does for the other two scenarios. Overall, the PHD performs very favorably to the clairvoyant filters despite the fact that the PHD is actually estimating the number of targets in the scene during each snapshot interval when the disc model is involved. Surprisingly, the clairvoyant PHD demonstrates little to no advantage over the PHD for any of the sensing model cases over all scenarios.

Figure 11 shows the average estimated number of targets versus snapshot time for the PHD filter for all four sensing model cases over all four scenarios. For the matching probabilistic case (Case 1), the PHD is able to accurately estimate the number of targets. When the PHD still uses the probabilistic model but the sensor behaviors follow the disc model, the PHD can still accurately estimate the target number as long as the targets are sufficiently spaced. When the targets are nearby, the sensing range of the sensors do not increase, and the size of the cluster of sensors detecting the sensors is consistent for a single target in the probabilistic model. Therefore, the PHD underestimates the number of targets. When the PHD employs the disc sensing model, the ambiguity issues related to the disc models makes it impossible for the PHD to accurately estimate the number of targets over all snapshots.

B. Effects of Innovative Particles, Motion Model, and Initialization

In all the simulations presented up to this point, about 9.09% of the multiobject particles are innovative ($J = 100$, $P_{ex} = 1100$). Some innovative particles are necessary to regulate against a small number of particles and/or a simple motion model. In the next set of simulations, J is allowed to vary to study the effect of the number of innovative particles on performance. Fig. 13 plots the performance of all three filters as percentage of the innovative particle when $P_{ex} = 1500$. This figure represents the matching probabilistic sensing case of Scenario A. Similar results were obtained over the other scenarios for sensing Case 1. Note that when $J = 1500$, all the multiobject particles are innovative, and the motion model is ignored. The filters are simply fusing the current set of binary sensor measurements to localize the targets. As J increases from zero to 1500, the filters are simply putting more confidence on the current measurements. The figure demonstrates that about 10% of innovative particles are sufficient to accurately estimate the number of targets and their locations. The performance degrades only slightly as the innovative percentage grows from 10% to 90%. The localization performance falls off by a factor of two when using all innovative particles. Thus, the tracking, i.e., incorporation of prior measurements, does provide for some performance advantages.

The good performance of using all innovative particles relative to using none implies that the proposal function to

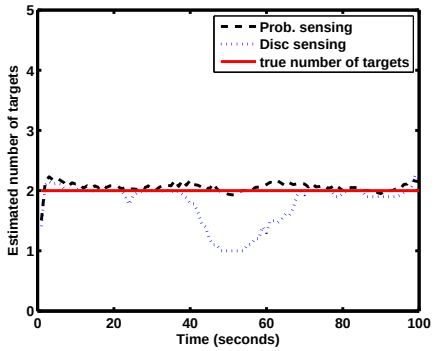

(a)

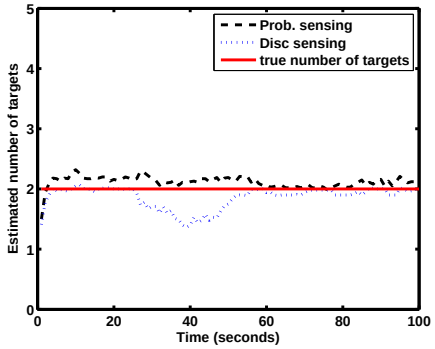

(b)

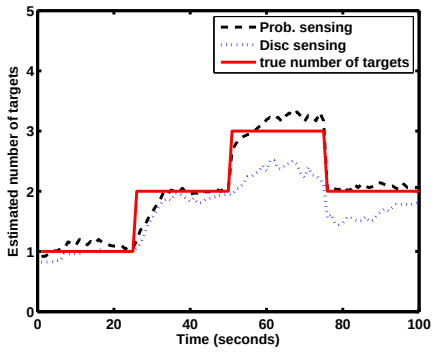

(c)

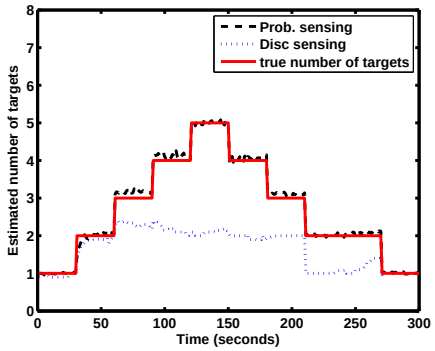

(d)

Fig. 11. When the filters implement probabilistic model, estimated number of targets using PHD for (a) Scenario A (b) Scenario B (c) Scenario C (d) Scenario D. The legends refer to the actual models adopted by the sensors. Note that for the matching probabilistic case, the average RMS error of the estimated number of targets over the whole observation period is 0.34, 0.38, 0.42 and 0.38 for Scenario A, B, C and D, respectively.

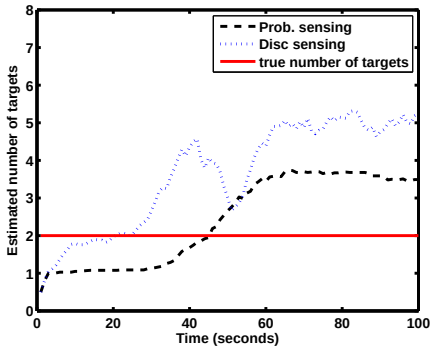

(a)

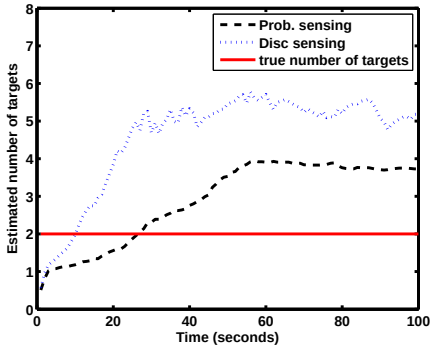

(b)

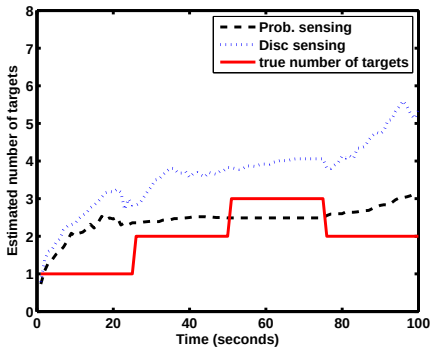

(c)

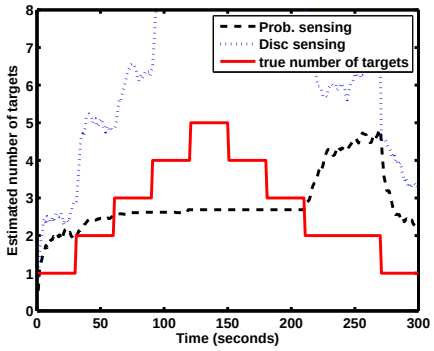

(d)

Fig. 12. When the filters implement disc model, estimated number of targets using PHD for (a) Scenario A (b) Scenario B (c) Scenario C (d) Scenario D. The legends refer to the actual models adopted by the sensors.

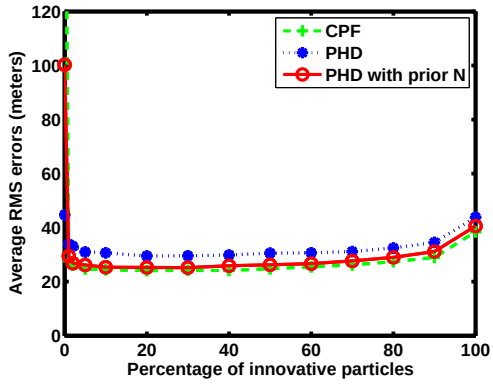

(a)

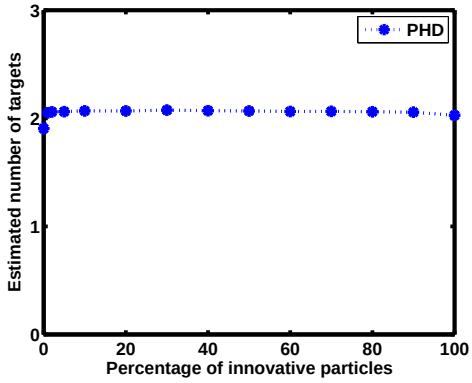

(b)

Fig. 13. For Scenario A and matching probabilistic case, (a) Average CA-OSPA errors (b) estimated number of targets, versus the percentage of innovative particles in PHD

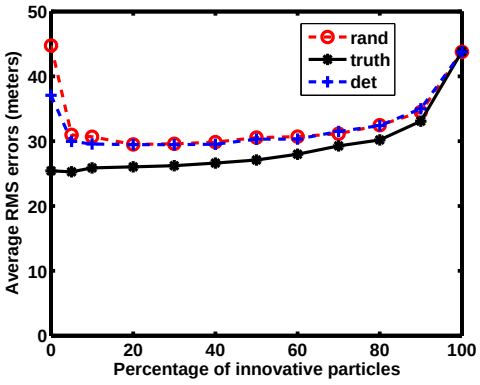

(a)

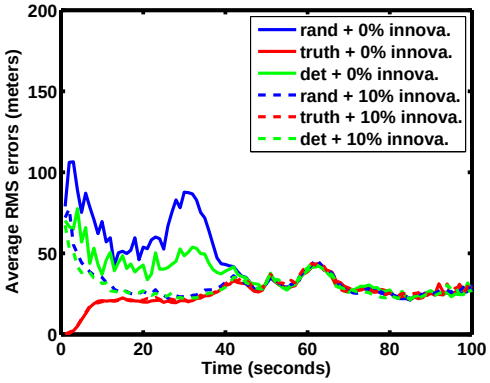

(b)

Fig. 14. For Scenario A and matching probabilistic case, PHD with random initialization, ground truth initialization, detecting sensor initialization (a). Average CA-OSPA errors versus the percentage of innovative particles; (b). Average CA-OSPA errors versus time when the innovative particles are either zero or 10 percent during tracking

obtain innovative particles is effective. To better understand the tradeoff between the prediction due to the target motion model and the innovation due to the current measurements, in Fig. 14, we compare PHDs for Scenario 1 and Case 1 when one uses the ground truth, the random samples in the whole field, and the random samples in the rectangular area bounding all detecting sensors as the initial PHD particles, respectively. Since in Scenario A, the targets are moving at a constant velocity, the ground truth initial 4-state PHD particles are the true target positions and velocities. For the random initialization case, the initial particles are random samples in the whole field. For the detecting sensor initialization case, the initial particles are random samples in the smallest rectangular bounding box surrounding the detecting sensors. It is clear that the ground truth initialization helps the most when there are no innovative particles. As the number of innovative particles increases, the advantages brought by the ground truth initialization become less obvious. When using the detecting initialization, the track filtering employing no innovative particles is as effective as employing all innovative particle. One still needs to use around 10% innovative particles for best localization performance. Note that the smaller range for the y-axis in Fig. 14(a) than in Fig. 13(a) shows that localization performance degrades slightly as the number of innovative particles increases from 10% to 90%. Finally, Fig. 14(b) demonstrates how good initialization and/or innovative particles enable the PHD filter to reach a steady state behavior.

C. Comparisons with ClusterTrack in 1-D

The next set of simulations compare the PHD against the instantiation of ClusterTrack as described in [8]. Unlike the PHD method, ClusterTrack returns particles representing possible tracks where a particle is the estimated location point of time at each snapshot interval. The initial iteration of ClusterTrack builds up the particles over time in a sequential fashion so that at time $t = T$ a particle represents the estimated location of a target from $t = 0$ to $t = T$ using data up to time T. ClusterTrack also assumes that the number of targets is constant and estimates the target number as the maximum number of feasible target regions over the entire surveillance time interval. Then, ClusterTrack uses multiple iterations to refine the particles so that feasible target regions are covered by the collection of particles. To this end, ClusterTrack does not account for appearance and disappearance of targets. Thus it can generate more particles than actual targets, and its ability to capture all targets depends on good parameter choices which are described in [8]. However, it is admitted in [8] that there is no theoretical guarantee that the ClusterTrack will catch all

the targets. Furthermore, ClusterTrack can only localize all targets after multiple iterations which is operating in a batch mode where measurements from future times are influencing the estimated target locations at earlier points in time.

In our simulations for the ClusterTrack method, we slightly modify code provided by the authors of [8] to accommodate for a test scenario since the original ClusterTrack assumed the number of targets in the scene remains constant. This first test reproduces the scenario in [8]: sensors are uniformly distributed in 1-D, the separation between consecutive sensors is equal to the sensing range, so that the coverage area for the adjacent sensors has 50 percent overlap. In this case, the number of sensors is 50, and the disc sensing range is 30, and the observation range is 1250. Fig. 15 shows that estimated target locations from the PHD filter and the ClusterTrack traces after one and two iterations. The PHD and ClusterTrack (after two iterations) are able to capture all targets. However, when ClusterTrack is behaving as a filter (and not a smoother) for the first iteration, it is unable to capture all the targets.

In the second comparison, the number of targets changes during the surveillance interval. Figure 16 shows that the PHD and ClusterTrack (after four iterations) are able to capture all the targets. Again, ClusterTrack fails to localize all the tracks after the first iteration. After multiple intervals, the traces in ClusterTrack will jump whenever targets are born or die. ClusterTrack forces these jumps as an artifact of its assumption that the number of targets is constant.

Overall, ClusterTrack is an effective multiple target tracker after a number of iterations, and the localization ability of the PHD and ClusterTrack appear to be comparable. However, the PHD can capture all targets as a track filter, while ClusterTrack requires multiple iterations working in a track smoothing mode to capture the targets. On the other hand, ClusterTrack does provide traces of the tracks, and the PHD only provides estimates of the target locations at each snapshot interval. Finally the method to build and refine particles in ClusterTrack assumes the disc model, and it is not clear how to modify ClusterTrack to consider the probabilistic sensing model. When incorporating the probabilistic sensing models, the PHD provides an accurate estimate of the number of targets at each snapshot interval when the probabilistic model actually represents the behavior of the sensors. ClusterTrack cannot provide for such an estimate.

D. Discussion

The simulations demonstrate that effectiveness of the proposed PHD method for multitarget tracking using proximity sensors. The PHD method appears to be more robust when employing the probabilistic sensing model than the disc model. Furthermore, the CPF filter can break down when employing the disc model. It appears that the weight update using probabilistic model is better than using the disc model because the probabilistic model accounts for the imperfect multiobject particles with non-zero weights. Here the imperfect multi-object particles refer to ones where some subparticles are good but the others are far from any ground truth target. Using an example in Fig. 17, we show the disadvantages

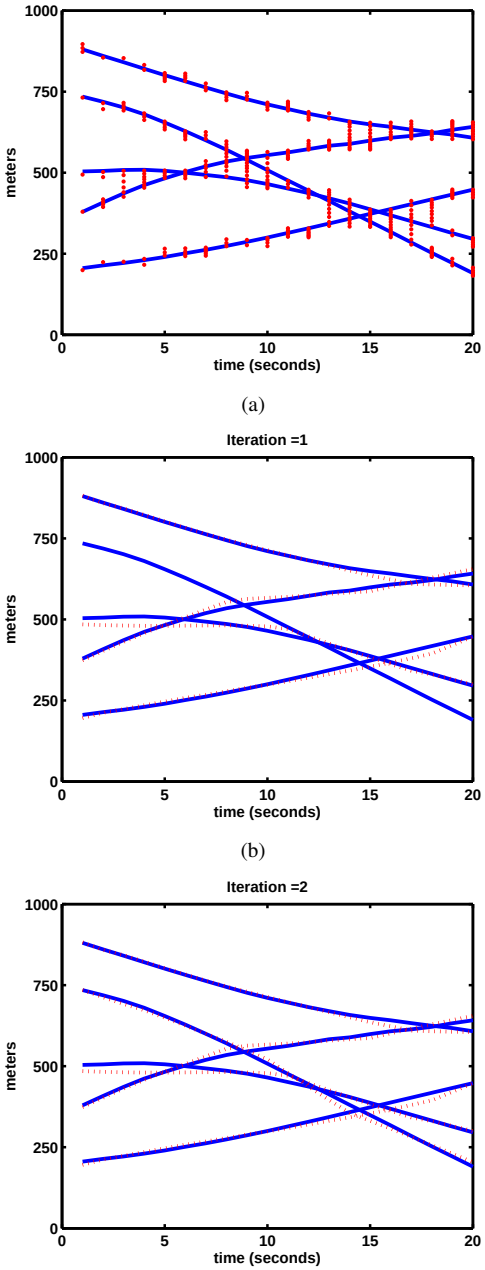

Fig. 15. For no target birth/death cases, (a). estimated target positions using PHD vs. time (b)-(c). at each iteration of ClusterTrack, positions of cluster heads vs. time, where true target tracks are in solid lines, and dots or dashed lines denote the estimates using either PHD or ClusterTrack method, respectively

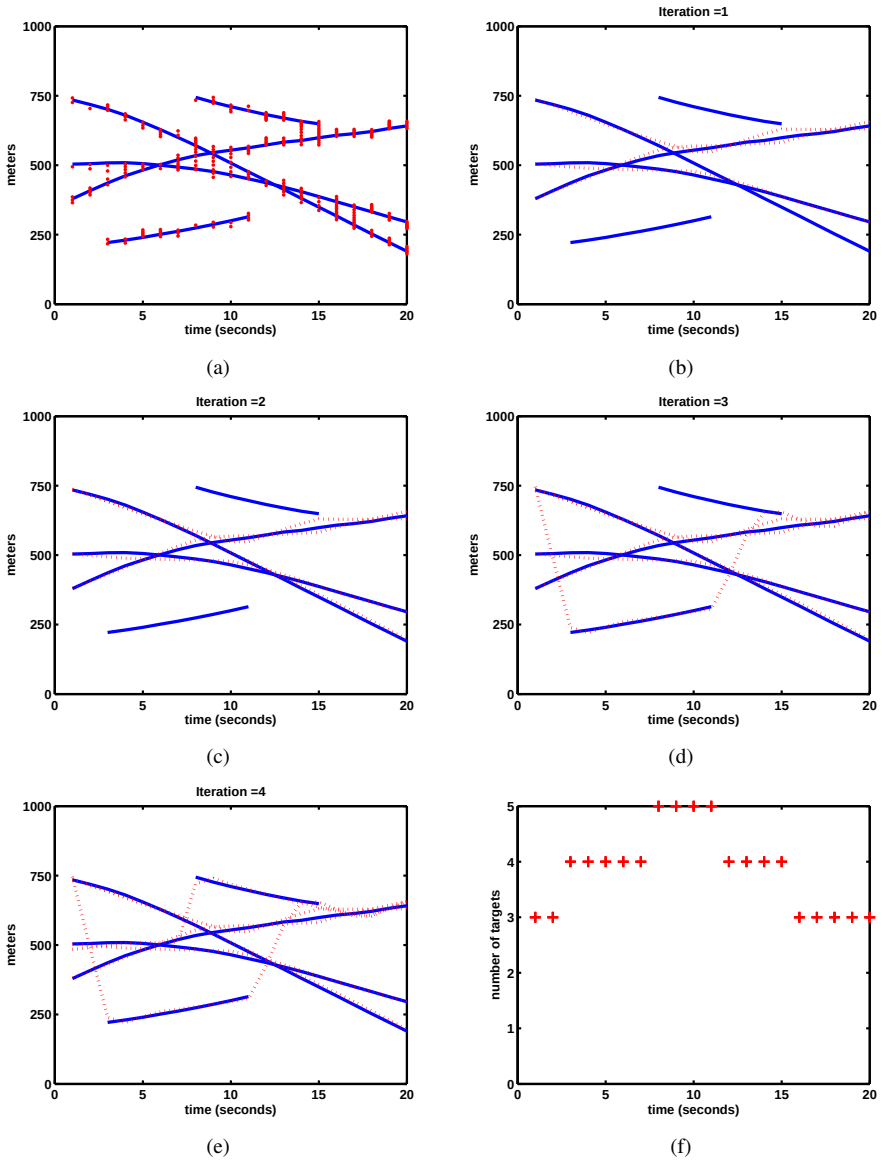

Fig. 16. For target birth/death cases, (a). estimated target positions using PHD vs. time (b)-(e). at each iteration of ClusterTrack, positions of cluster heads vs. time, where true target tracks are in solid lines, and dots or dashed lines denote the estimates using either PHD or ClusterTrack method, respectively. (f). the number of targets versus time

of assuming the disc model in the measurement update for the filters. Following the measurement update, it is desirable for the weights associated to imperfect particles to be greater than zero since some portion of its subparticles are good. However in the disc model, for the weights to be nonzero, all subparticles associated to the multiobject have to lie beyond the sensing radius of any non-detecting sensor, and there must be at least one subparticle within the detection range of all detecting sensors (see (5) and (13)). For example, among the five sensors in Fig. 17, three sensors centered in the shaded circles report target detections. Suppose there are three multiobject particles, each denoted by the stars, pluses, and diamonds, respectively. The weights for the star, plus and diamond multitargets are 0, 1, and 0, respectively, when using (5) and (13). The weight for the star particles is zero because there is a subparticle that lies within sensing range of non-detecting Sensor 4. The weight for the diamond particles is also zero because there is no subparticle that lies within the sensing range of sensor 3. When using the bounding box to generate innovative particles, there is a high chance that none have positive weights for the disc model when the targets are far apart.

On the contrary, the weights generated by the probabilistic model for the imperfect star and diamond particles are nonzero. Overall, the probabilistic model does a better job of rating the overall goodness of a particle as the weight is not binary. Furthermore, the probabilistic model does not prune particles that contain good subparticles. These good subparticles can lead to good solutions, and the crossover feature of the PHD allows good subparticles from otherwise weak particles to combine into strong particles.

When the number of targets grows to three or more, the

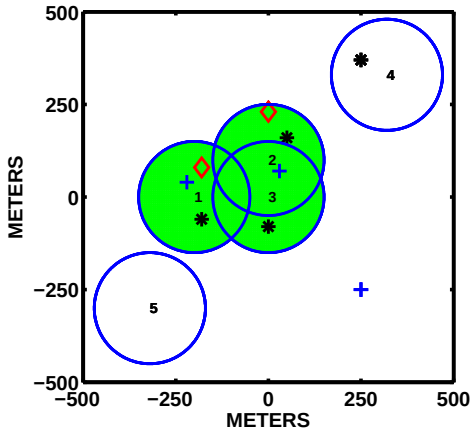

Fig. 17. Illustration of weight updates using the disc model where sensors{1,2,3} report $d_i^t = 1$ and sensors{4,5} report $d_i^t = 0$. The weights for the star, plus and diamond multitargets are 0, 1, and 0, respectively, when using the disc model, i.e., (5) and (13)

localization accuracy of the PHD degrades for all four cases. However, for Case 1 (matching probabilistic model), the PHD is able to accurately track the number of targets. It is interesting to note that for Case 4, the filter underestimates the number of targets for Scenarios C and D once the number of targets grows to three or more (see Figure 11). Since the PHD filter is employing the probabilistic model, the underestimation is caused by targets that are too close to each other to create large enough clusters of detections indicative of the true number of targets. As a result, the particles of the PHD will coalesce into a smaller number of clusters than targets for any of the four cases, and this will create problems for the k-means algorithm to determine which PHD particles should belong to which targets. Overall, the centroid for the partitions may not be reflective of the ground truth targets. Future work should investigate whether alternative clustering method [29], [30], [31] can improve the localization.

In all simulations in Section IV-A, the clairvoyant PHD does not clearly outperform the PHD. This was unexpected given that the clairvoyant filter always forces $n^{(k)}$ in Step 3 of the PHD (see Figure 2) to equal the ground truth number of targets. The clairvoyant PHD does slightly outperform the PHD for the matching probabilistic sensing case for all scenarios except Scenario D, when four or more targets enter the scene. Inspection of Figure 11 indicates that the PHD slightly overestimates the number of targets for that case, which means more of the P^* PHD particles after collapsing the multiobject density (see (23)) represent good solutions for the PHD filter than for the clairvoyant PHD filter. This larger diversity of good PHD particles might translate to better localization. In fact, forcing $n^{(k)}$ to equal the ground truth target number does constrain the search for good multiobject particles with high likelihood, i.e., good hypotheses that explain the sensor measurements, and may offer little to no advantages when the sensor/target configuration is such that the target count is ambiguous. Thus, the PHD filter can outperform the clairvoyant PHD filter in cases where the disc model is considered.

Finally, the capability for the PHD methods to estimate the number of targets for Case 1 is not boundless. As more targets enter in the scene a higher percentage of sensors will report detections. For the case of five targets (using the probabilistic sensing model), thirty percent of the sensors generate detections. When the number of targets grows to twenty, all hundred sensors will normally return detections. In this extreme case, the ability to localize the targets completely disappears as any configuration of twenty targets will be sensed by all sensors. To accurately localize targets, a certain number of non-reporting sensors are required. Perhaps, this issue also affects the poorer localization performance in Scenarios C and D when targets move too close to each other. The resolution problem does not appear for two or less targets as seen in these simulations and in the results of [21] that specifically investigated the resolution issue. Future work can investigate the resolution limits of the PHD filter for three or more targets.

V. Conclusions

This work documents our investigation of multiple target tracking filters in proximity sensor networks. To this end, we developed a novel formulation of the PHD filter for proximity sensors. We compared the PHD against two clairvoyant filters that assume the number of targets is known a priori. For measuring the localization errors, we considered a measure that attempts to separate out the effects of cardinality errors. The simulations show the advantages of the crossover feature in the PHD.

Two possible measurement models were considered: the disc and probabilistic, so that two model matching cases and two model mismatching cases were considered. While the disc model has wide appeal, the probabilistic model better represents the phenomenology that dictates how sensors respond to target signals. The simulations demonstrate that the PHD filter would be unable to accurately estimate the number of targets if the disc model was assumed in the measurement update. This is the case because the hypothesis that explains the pattern of detection reports is not unique. On the other hand, the PHD is accurate when using the probabilistic model in the measurement update because of the uniqueness of the best hypothesis to explain the pattern of detection reports.

The unique hypothesis emerges because it is assumed that the radiating power of each target is a fixed and known quantity. In reality, one would expect that this power fluctuates from target to target. If these fluctuations are unbounded, the probabilistic model becomes completely ambiguous, and it would be impossible for the PHD filter to accurately estimate the number of objects in the scene. However, we expect that these fluctuations are bounded. Future work will investigate how allowing for bounded spread of target power levels will affect the performance of the PHD filter. Other future work will investigate better dynamical models to improve the tracking performance including target motion and birth/death models, and other cluster methods for closely spaced targets.

Finally, the new PHD filter in this paper uses a profoundly different measurement model than the traditional PHD filter.

When the sensor measurements are statistically independent conditioned on the target hypothesis as in this paper, the multisensor version of the PHD is straightforward. However, for the traditional PHD filter, the "exact" multisensor version is very cumbersome to implement [32]. Usually, approximations are incorporated in the multisensor implementation of the traditional PHD. These approximations are necessary due to the constraints that a measurement corresponds either to one unique target or clutter. Actually, the measurements are usually derived from raw signals through signal processing, e.g., direction of arrival estimation. As an alternative, the new PHD method could easily be modified to consider the likelihood of raw signals given the target hypotheses. The new PHD method does suffer from approximations in the particle implementation of the multiobject target density. On the other hand, approximations of the PHD for sensor fusion also lead to performance loss. Future work can investigate whether the new PHD method operating over raw signals from multiple sensors has utility compared to multiple sensor implementation of the traditional PHD method.

VI. ACKNOWLEDGMENTS

The authors wish to thank Dr. Jaspreet Singh and Prof. Upamanyu Madhow for providing the source code to implement ClusterTrack as described in [8]. We also thank the reviewers for their helpful and insightful comments on the early draft of the paper.

REFERENCES

[1] A. Artes-Rodriguez, M. Lazaro, and L. Tong, "Target location estimation in sensor networks using range information," in *IEEE Sensor Array and Multichannel Signal Processing workshop*, 2004.

[2] P. Djuric, M. Vemula, and M. Bugallo, "Target tracking by particle filtering in binary sensor networks," *IEEE Trans. on Signal Processing*, vol. 56, no. 6, pp. 2229–2238, 2008.

[3] W. Kim, K.Mechitov, J.Choi, and S.Ham, "On target tracking with binary proximity sensors," in *Proceedings of ACM/IEEE IPSN*, 2005.

[4] J. Aslam, Z. Butler, F. Constantin, V. Crespi, G.Cybenko, and D. Rus, "Tracking a moving object with a binary sensor network," in *Proceedings of ACM SensSys*, 2003.

[5] N. Shrivastava, R. Mudumbai, U. Madhow, and S. Suri, "Target tracking with binary proximity sensors," *ACM Trans. on Sensor Networks*, vol. 5, no. 4, Nov. 2009.

[6] Z. Wang, E. Bulut, and B. K. Szymanski, "Distributed energy-efficient target tracking with binary sensor networks," *ACM Trans. on Sensor Networks*, vol. 6, no. 4, Jul. 2010.

[7] J. Singh, U. Madhow, R. Kumar, S. Suri, and R. Cagley, "Tracking multiple targets using binary proximity sensors," in *Proceedings of IPSN*, 2007.

[8] J. Singh, R. Kumar, U. Madhow, S. Suri, and R. Cagley, "Multiple-target tracking with binary proximity sensors," *ACM Trans. on Sensor Networks*, vol. 8, no. 1, Aug. 2011.

[9] T. He, C. Bisdikian, L. Kaplan, W. Wei, and D. Towsley, "Multi-target tracking using proximity sensors," in *Proc. of the Military Communications Conference (MILCOM)*, San Jose, CA, Nov. 2010.

[10] Q. Le and L. M. Kaplan, "Target localization using proximity binary sensors," in *Proc. of the IEEE Aerospace Conference*, Big Sky, MT, Mar. 2010.

[11] R. Mahler, "Multi-target Bayes filtering via first-order multi-target moments," *IEEE Trans. on Aerospace and Electronic Systems*, vol. 39, no. 4, pp. 1152–1178, 2003.

[12] Y. Bar-Shalom and X. Li, *Estimation and Tracking: Principles, Techniques, and Software*. Boston: Artech House, 1993.

[13] B. T. Vo, S. Singh, and A. Doucet, "Sequential Monte Carlo methods for multi-target filtering with random finite sets," *IEEE Trans. on Aerospace and Electronic Systems*, vol. 41, no. 4, pp. 1224–1245, 2005.

[14] D. E. Clark and J. Bell, "Bayesian multiple target tracking in forward scan sonar images using the PHD filter," in *Proc. of the IEE Radar, Sonar and Navigation*, vol. 152, 2005, pp. 327–334.

[15] D. E. Clark, I. Ruiz, Y. Petillot, and J. Bell, "Particle PHD filter multiple target tracking in sonar image," *IEEE Trans. on Aerospace and Electronic Systems*, vol. 43, no. 1, pp. 409 –416, january 2007.

[16] Y.-D. Wang, J.-K. Wu, A. Kassim, and W. Huang, "Data-driven probability hypothesis density filter for visual tracking," *IEEE Transactions on Circuits and Systems for Video Technology*, vol. 18, no. 8, pp. 1085 – 1095, 2008.

[17] M. Tobias and A. Lanterman, "Probability hypothesis density-based multitarget tracking with bistatic range and Doppler observations," in *Proc. of the IEE Radar, Sonar and Navigation*, vol. 152, 2005, pp. 195 – 205.

[18] B. T. Vo, B.N.Vo, and A. Cantoni, "Analytic implementations of the cardinalized probability hypothesis density filter," *IEEE Trans. on Signal Processing*, vol. 55, no. 7, pp. 3553–3567, 2007.

[19] Q. Le and L. M. Kaplan, "Multitarget tracking using proximity sensors," in *Proc. of the 27th Army Science Conference*, Orlando, FL, Nov. 2010.

[20] ——, "Target tracking using proximity binary sensors," in *Proc. of the IEEE Aerospace Conference*, Big Sky, MT, Mar. 2011.

[21] ——, "Effects of operation parameters on multitarget tracking in proximity sensor networks," in *Proc. of the SPIE*, vol. 8050, Apr. 2011.

[22] X. Sheng and Y.H.Hu, "Maximum likelihood multiple-source localization using acoustic energy measurements with wireless sensor networks," *IEEE Trans. on Signal Processing*, vol. 53, no. 1, pp. 44 – 53, 2005.

[23] Y. Bar-Shalom, X. R. Li, and T. Kirubarajan, *Estimation with Applications to Tracking and Navigation: Theory, Algorithms, and Software*. New York: John Wiley & Sons, Inc., 2001.

[24] R. L. Streit, *Poisson Point Processes: Imaging, Tracking, and Sensing*. New York: Springer, 2010.

[25] W. K. Hastings, "Monte Carlo sampling methods using Markov chains and their applications," *Biometrika*, vol. 57, no. 1, pp. 97–109, Apr. 1970.

[26] K. R. Pattipati, T. Kirubarajan, and R. L. Popp, "Survey of assignment techniques for multitarget tracking," in *Multitarget-Multisensor Tracking: Applications and Advances*, Y. Bar-Shalom and W. D. Blair, Eds., vol. 3. Norwood, MA: Artech House, 2000, pp. 77–159.

[27] J. Hoffman and R. Mahler, "Multitarget miss distance via optimal assignment," *IEEE Trans. on System, Man, and Cybernetic*, vol. 34, no. 3, pp. 327 – 336, 2004.

[28] S. Dominic, B. Vo, and B. Vo, "A consistent metric for performance evaluation of multi-object filters," *IEEE Trans. on Signal Processing*, vol. 43, no. 2, pp. 556 – 570, 2008.

[29] L. Lin, B.-S. Y., and T. Kirubarajan, "Track labeling and PHD filter for multitarget tracking," *IEEE Trans. on Aerospace and Electronic Systems*, vol. 42, no. 3, pp. 778 – 795, 2006.

[30] B.N.Vo and W.K.Ma, "The Gaussian mixture probability hypothesis density filter," *IEEE Trans. on Signal Processing*, vol. 54, no. 11, pp. 4091–4104, 2006.

[31] B. Ristic, D. Clark, and B.-N. Vo, "Improved SMC implementation of the PHD filter," in *Proc. of Information Fusion*, Edingburgh, Scottland, Jul. 2010.

[32] R. Mahler, "The multisensor PHD filter: I. general solution via multi-target calculus," in *Proc. of the SPIE*, vol. 7336, Apr. 2009.

Qiang Le received Ph.D. in Electrical and Computer Engineering at Georgia Institute of Technology in 2006. In August 2006, she joined Hampton University as an assistant professor in Electrical Engineering. Her current research interests include multiple target tracking, sensor fusion for target localization, sensor management in wireless sensor network, signal detection and estimation, and engineering education research. Her research has been awarded by ARL and her collaborative work on engineering education research was awarded by NSF.

Lance M. Kaplan received the B.S. degree with distinction from Duke University, Durham, NC, in 1989 and the M.S. and Ph.D. degrees from the University of Southern California, Los Angeles, in 1991 and 1994, respectively, all in Electrical Engineering. From 1987-1990, Dr. Kaplan worked as a Technical Assistant at the Georgia Tech Research Institute. He held a National Science Foundation Graduate Fellowship and a USC Dean's Merit Fellowship from 1990-1993, and worked as a Research Assistant in the Signal and Image Processing Institute at the University of Southern California from 1993-1994. Then, he worked on staff in the Reconnaissance Systems Department of the Hughes Aircraft Company from 1994-1996. From 1996-2004, he was a member of the faculty in the Department of Engineering and a senior investigator in the Center of Theoretical Studies of Physical Systems (CTSPS) at Clark Atlanta University (CAU), Atlanta, GA. Currently, he is a researcher in the Networked Sensing and Fusion branch of the U.S. Army Research Laboratory. Dr. Kaplan serves as Editor-In-Chief for the IEEE Transactions on Aerospace and Electronic Systems (AES). In addition, he also serves on the Board of Governors of the IEEE AES Society and on the Board of Directors of the International Society of Information Fusion. He is a three time recipient of the Clark Atlanta University Electrical Engineering Instructional Excellence Award from 1999-2001. His current research interests include signal and image processing, automatic target recognition, information/data fusion, and resource management.

LE QIANG

From: taes@msubmit.net
Sent: Tuesday, September 11, 2012 12:31 PM
To: LE QIANG
Cc: lkaplan@ieee.org; rjanssen@allenpress.com
Subject: TAES-201100630R Decision Letter

"Probability Hypothesis Density-Based Multitarget Tracking for Proximity Sensor Networks"

Dear Dr. Le:

On behalf of the IEEE Transactions on Aerospace and Electronic Systems (TAES), I am pleased to accept your above referenced manuscript for publication. The IEEE AESS Editorial Office will contact you with the requirements for your Final Submission Package, and you timely response will minimize publication delays.

Please note that the reviewers have made some additional comments that you should address in your final upload. I do not think that your response needs to be checked by me or the reviewers, they are intended for clarification.

Please note that if your manuscript was first submitted November 1 of 2010 or later you have agreed to our mandatory page-charge policy: $200 for every printed page beyond 10 (for a regular paper) and beyond 6 (for a correspondence); and $250 for every page in a "Letter".

As an alternative, the author should be aware that the IEEE offers Open Access publishing through an option that allows authors to designate whether their articles should be provided as Open Access: that is, freely available to any visitor to IEEE Xplore. Authors who choose open access must do so by electing this option by notifying the Editor-In-Chief. A mandatory fee of $3,000 will be billed at the time of publication to support publishing costs. For any questions regarding IEEE's Open Access policy, please refer to IEEE's Frequently Asked Questions on Open Access.

In some cases a manuscript was initially submitted as a regular paper but has been accepted as a correspondence item; this may result in an increase in the mandatory page charges. You may reduce the length, but if this requires significant modification you must contact the accepting Associate Editor for approval, as the accepted and final manuscripts will be cross-checked.

Thank you for your contribution to the IEEE Transactions on Aerospace and Electronic Systems.

Sincerely,

Peter Willett
Editor in Chief
IEEE Transactions on Aerospace and Electronic Systems

Reviewer #1 (Remarks to the Author - Is the title appropriate, such that someone doing related research would discover this article in an automated search, such as via IEEEXplore?):

Yes